

Aging in one-dimensional coagulation-diffusion processes and the Fredrickson-Andersen model

Peter Mayer¹ and Peter Sollich²

¹ Department of Chemistry, Columbia University, 3000 Broadway, New York, NY 10027, USA

² King's College London, Department of Mathematics, Strand, London WC2R 2LS, UK

E-mail: pm2214@columbia.edu and peter.sollich@kcl.ac.uk

Abstract. We analyse the aging dynamics of the one-dimensional Fredrickson-Andersen (FA) model in the nonequilibrium regime following a low temperature quench. Relaxation then effectively proceeds via diffusion limited pair coagulation (DLPC) of mobility excitations. By employing a familiar stochastic similarity transformation, we map exact results from the free fermion case of diffusion limited pair annihilation to DLPC. Crucially, we are able to adapt the mapping technique to averages involving multiple time quantities. This relies on knowledge of the explicit form of the evolution operators involved. Exact results are obtained for two-time correlation and response functions in the free fermion DLPC process. The corresponding long-time scaling forms apply to a wider class of DLPC processes, including the FA model. We are thus able to exactly characterise the violations of the fluctuation-dissipation theorem (FDT) in the aging regime of the FA model. We find nontrivial scaling forms for the fluctuation-dissipation ratio (FDR) $X = X(t_w/t)$, but with a *negative* asymptotic value $X^\infty = -3\pi/(6\pi - 16) \approx -3.307$. While this prevents a thermodynamic interpretation in terms of an effective temperature, it is a direct consequence of probing FDT with observables that couple to activated dynamics. The existence of negative FDRs should therefore be a widespread feature in non mean-field systems.

PACS numbers: 05.70.Ln, 05.40.-a, 64.70.Pf, 75.40.Gb

Introduction

A generic feature of glass-formers is the rapid increase of their relaxation time with decreasing temperature. When quenched below the laboratory glass transition, where relaxation times exceed experimental timescales, these systems fall out of equilibrium. They change from equilibrated fluids to nonequilibrium amorphous solids [1]. The “waiting time” t_w elapsed since preparation of the state then sets a timescale for the subsequent relaxation: the system ages [2]. A full understanding of this nonequilibrium phenomenon remains a central theoretical challenge.

Mean-field models of structural and spin glasses [3, 4], in which relaxation times strictly diverge at the glass transition, have delivered important insights into the dynamics of aging. Most notably, these systems satisfy a generalized fluctuation-dissipation theorem (FDT) in their nonequilibrium, aging state. This is defined in terms of the two-time connected correlation function for a generic observable A ,

$$C(t, t_w) = \langle A(t)A(t_w) \rangle - \langle A(t) \rangle \langle A(t_w) \rangle, \quad (1)$$

with $t \geq t_w$, and the corresponding two-time response function

$$R(t, t_w) = T \left. \frac{\delta \langle A(t) \rangle}{\delta h(t_w)} \right|_{h=0}. \quad (2)$$

Here h denotes the thermodynamically conjugate field to the observable A so that the perturbation of the Hamiltonian is $\delta \mathcal{H} = -hA$. Note that we have absorbed the temperature T in the definition of the response. The associated generalized FDT is then

$$R(t, t_w) = X(t, t_w) \frac{\partial}{\partial t_w} C(t, t_w), \quad (3)$$

with $X(t, t_w)$ the fluctuation-dissipation ratio (FDR). At equilibrium, correlation and response functions are time translation invariant, depending only on $\Delta t = t - t_w$, and equilibrium FDT imposes that $X = 1$. This is no longer true in nonequilibrium systems. But the definition of an FDR through Eq. (3) becomes nontrivial for aging systems: in the mean-field spin glass models [3, 4] its dependence on both time arguments is only through the correlation function $X(t, t_w) \sim X(C(t, t_w))$ at large times. This led to the introduction of timescale dependent effective temperatures [5], and a possible thermodynamic interpretation of aging [3, 4, 6].

In many systems of physical interest, however, such as liquids quenched below the glass transition or domain growth in disordered magnets [7], the dynamics is not of mean-field type. Crucial new features are activated processes and spatial heterogeneity [8, 9, 10, 11]. Some experiments and simulations [12] have nonetheless seemed to detect a mean-field aging regime. On the other hand, theoretical studies have found ill-defined FDRs [13, 14], non-monotonic response functions [15, 16, 17, 18], observable dependence [19, 20], nontrivial FDRs without thermodynamic transitions [21, 22] and a subtle interplay between growing dynamical correlation lengthscales and FDT violations [23, 24]. Also in experiments deviations from mean-field expectations have been observed, with for example anomalously large FDT violations associated with

intermittent dynamics [25]. It thus remains an important task to delineate when the mean-field concept of an FDR-related effective temperature remains viable.

In this paper, we focus on the one-dimensional Fredrickson-Andersen (FA) model [26, 27]. Its relaxation time follows an Arrhenius law at low temperatures, and it is the simplest kinetically constrained model for glassy systems which displays dynamical heterogeneity [28, 29, 30, 31]. We use it to study systematically the impact of activated, and in this sense strongly non mean-field, dynamics on FDRs and associated effective temperatures. In addition, the FA model dynamics become critical at low temperatures [32, 33, 34], with a diverging dynamical lengthscale. Our work is also of relevance, therefore, to the study of FDRs in nonequilibrium critical dynamics. Here, FDRs play the role of universal amplitude ratios, which makes them important markers for distinguishing dynamic universality classes [35].

A first numerical study of FDT violation in the one-dimensional FA model appeared in [13] and suggested ill defined FDRs. The authors used disconnected correlations, however, which compromises their results since FDT would not be recovered in equilibrium. More recent numerical studies [21, 36] based on the correct, connected correlations indicate a very different picture: *no* detectable violation of the equilibrium FDT is observed in spite of the nonequilibrium aging dynamics. We show below that this is a consequence of the specific scaling in the quasi-equilibrium regime [37], which acts to obscure genuine aging contributions. These contributions are nevertheless present as we will show, leading to FDT violations with well-defined FDRs in the activated aging regime of the FA model. We take advantage of observable dependence of the FDR in order to gain more direct access to FDT violations, by considering global rather than local observables. Our discussion also elucidates the physical origin of negative dynamical response functions, and predicts the generic existence of negative FDRs for observables directly coupled to activated processes. A partial summary of our results can be found in [38].

Our analysis of aging in the FA model is based on a close connection with diffusion limited pair coagulation (DLPC) processes. The research field of diffusion limited reaction processes is well developed [39] and offers powerful analytical tools [40, 41]. These include, in particular, stochastic similarity transformations [42, 43]. We use the latter to map exact results for the free fermion case of diffusion limited pair annihilation (DLPA) to DLPC. In particular, we show how the mapping technique can be adapted to averages involving multiple time quantities. This relies on knowledge of the explicit form of the evolution operators involved. We derive simple and explicit propagators for certain observables in DLPA and DLPC. In the free fermion DLPC process this yields new and exact results, for instance, the two-time particle correlation functions. Our propagators are of generic value for the analysis of DLPA and DLPC, however, and could serve in further studies of these processes.

The paper is organized as follows: in Sec. 1 we recall the definition of the FA model and introduce the matrix formalism used throughout this manuscript. A discussion of the dynamics in the different stages of relaxation is given, and we establish the

connection to DLPC. The mapping between DLPC and DLPA is then stated in Sec. 2. We introduce suitable sets of observables, which are related in a simple manner by the mapping, and give expressions for their dynamics in the free fermion processes. Arguments are presented that establish the broader validity of the predictions for the long-time scaling behaviour. The generalisation of the mapping procedure to multiple time averages and propagators is presented in Sec. 3. Using the DLPC propagator, expressions for two-time correlation and response functions are derived in Sec. 3.1 and Sec. 3.2. Response functions in the FA model comprise two contributions representing different physical effects and correspondingly Sec. 3.2 is split into two subsections. Readers more interested in results than in their derivation may skip Sec. 2 and Sec. 3 on first reading, except for the beginning of Sec. 3.2 where our decomposition of response functions is introduced. Results for FDT violation in the activated aging regime of the FA model are then presented in Sec. 4 and Sec. 5 and deal with local and global observables, respectively. Each of these sections comprises three subsections, discussing separately the dynamics of correlations, response functions and the resulting FDRs. We conclude with a summary and discussion of our results in Sec. 6. Two short appendices contain useful mathematical and technical material.

1. Matrix Formalism

In this section we summarize the background for our subsequent analysis of the aging dynamics in the FA model. After recalling the definition of the FA model we review the standard operator formalism widely used in the literature for studying reaction diffusion problems. We then translate the FA model into this representation and discuss its effective dynamics in the different stages of relaxation after a quench.

The one-dimensional FA model [26] is defined on a linear lattice of size N subject to periodic boundary conditions. Assigned to each site i is a binary variable $n_i \in \{0, 1\}$, with $n_i = 1$ representing a mobile fluid region and $n_i = 0$ an immobile one. The state of the system is characterised by $\mathbf{n} = (n_1, n_2, \dots, n_N)$. The probability $p(\mathbf{n}, t)$ of being in state \mathbf{n} at time t evolves according to the generic master equation

$$\partial_t p(\mathbf{n}, t) = \sum_{\mathbf{n}'} [w(\mathbf{n}' \rightarrow \mathbf{n})p(\mathbf{n}', t) - w(\mathbf{n} \rightarrow \mathbf{n}')p(\mathbf{n}, t)], \quad (4)$$

where ∂_t denotes the time derivative and $w(\mathbf{n} \rightarrow \mathbf{n}')$ the rate for transitions from state \mathbf{n} to \mathbf{n}' . In the FA model these transition rates are given by

$$w(\mathbf{n} \rightarrow \mathbf{n}') = \sum_i f_i(\mathbf{n}) w_i(\mathbf{n}) \delta_{n_i, 1-n'_i} \prod_{j \neq i} \delta_{n_j, n'_j}. \quad (5)$$

The Kronecker deltas, $\delta_{n, n'} = 1$ if $n = n'$ and zero otherwise, express that transitions occur only between states \mathbf{n}, \mathbf{n}' differing by a single flip $n_i \rightarrow 1 - n_i$. Under Glauber dynamics at temperature T the (unconstrained) flip-rates are

$$w_i(\mathbf{n}) = \varepsilon(1 - n_i) + (1 - \varepsilon)n_i, \quad (6)$$

and obey detailed balance with respect to the noninteracting Hamiltonian $\mathcal{H} = \sum_i n_i$. Here $\varepsilon = \langle n_i \rangle = 1/(1 + e^{1/T})$ is the equilibrium density of mobility excitations; at low temperatures this is small and so the excitations can also be thought of as defects. The key ingredient of the FA model is the kinetic constraint

$$f_i(\mathbf{n}) = n_{i-1} + n_{i+1}. \quad (7)$$

The dynamics on each site i require facilitation by an adjacent mobility excitation $n_{i-1} = 1$ or $n_{i+1} = 1$. Since $f_i(\mathbf{n})$ is independent of n_i it preserves detailed balance; the equilibrium state of the FA model is trivial. However, the kinetic constraint induces nontrivial relaxation dynamics with a rich phenomenology including dynamical heterogeneity [28, 29, 30, 31, 32, 33, 34, 44, 45, 46].

The discussion throughout this manuscript is based on a standard operator formalism. In the following we briefly summarize the main ideas; more details may be found in [40, 43]. One associates with each site i two orthonormal states $|0\rangle$ and $|1\rangle$, or $|n_i\rangle$ for short, representing the mobility n_i . Then an orthonormal basis for the configuration space of the entire system is

$$|\mathbf{n}\rangle = \bigotimes_i |n_i\rangle \quad \text{with} \quad \langle \mathbf{n} | \mathbf{n}' \rangle = \prod_i \delta_{n_i, n'_i}. \quad (8)$$

Probabilistic states $|P(t)\rangle$ are defined by

$$|P(t)\rangle = \sum_{\mathbf{n}} p(\mathbf{n}, t) |\mathbf{n}\rangle, \quad (9)$$

from which the probability for any particular configuration \mathbf{n} is extracted via $p(\mathbf{n}, t) = \langle \mathbf{n} | P(t) \rangle$. One now multiplies the master equation Eq. (4) by $|\mathbf{n}\rangle$ and takes a sum over \mathbf{n} . The result may be cast in the form

$$\partial_t |P(t)\rangle = W |P(t)\rangle, \quad (10)$$

with W the master operator

$$W = \sum_{\mathbf{n}, \mathbf{n}'} w(\mathbf{n} \rightarrow \mathbf{n}') (|\mathbf{n}'\rangle \langle \mathbf{n}| - |\mathbf{n}\rangle \langle \mathbf{n}|). \quad (11)$$

Conservation of probability is compactly expressed by $\langle e | P(t) \rangle = 1$ if one introduces

$$\langle e | = \sum_{\mathbf{n}} \langle \mathbf{n} | = (\langle 0 | + \langle 1 |)^{\otimes N}. \quad (12)$$

This is the bra ground state of W because $\langle e | W = 0$ from Eq. (10). The corresponding ket ground state is by definition the equilibrium state $|P_{\text{eq}}\rangle$ so that W is generally a non-hermitian operator. The formal solution of Eq. (10) for initial state $|P(0)\rangle$ is

$$|P(t)\rangle = e^{Wt} |P(0)\rangle, \quad (13)$$

with e^{Wt} the evolution operator. To calculate the expectation value of an observable $A(\mathbf{n})$ one introduces the associated operator $A = \sum_{\mathbf{n}} A(\mathbf{n}) |\mathbf{n}\rangle \langle \mathbf{n}|$ in terms of which

$$\langle A(t) \rangle = \langle e | A | P(t) \rangle. \quad (14)$$

It is straightforward to verify that indeed $\langle e|A|P(t)\rangle = \sum_{\mathbf{n}} A(\mathbf{n})p(\mathbf{n}, t)$. This completes our recap of the operator formalism.

The FA master operator W^{FA} is obtained by substituting the transition rates Eq. (5) into Eq. (11). To state it explicitly it is useful to introduce the number operator

$$\hat{n}_i = \sum_{\mathbf{n}} n_i |\mathbf{n}\rangle \langle \mathbf{n}| = (|1\rangle \langle 1|)_i. \quad (15)$$

The notation $(X)_i$ indicates that the operator X lives in the subspace of site i , that is, $(X)_i = 1^{\otimes(i-1)} \otimes X \otimes 1^{\otimes(N-i)}$ with $1 = |0\rangle \langle 0| + |1\rangle \langle 1|$ the diagonal operator; we will not distinguish the identity operator 1 from the number 1 in our notation as the meaning is always clear from the context. We also introduce the flip operator

$$F_i = (|1\rangle \langle 0| + |0\rangle \langle 1|)_i, \quad (16)$$

which maps states $|\mathbf{n}\rangle$ onto $F_i |\mathbf{n}\rangle = |n_1, \dots, n_{i-1}, 1 - n_i, n_{i+1}, \dots, n_N\rangle$. It is important to note that F_i and \hat{n}_i do not commute. But of course $[F_i, \hat{n}_j] = 0$ if $i \neq j$ since both operators act locally. Other obvious and useful properties are $\hat{n}_i^2 = \hat{n}_i$ and $F_i^2 = 1$. The FA master operator now reads

$$W^{\text{FA}} = \sum_i (F_i - 1) f_i w_i, \quad (17)$$

where $f_i = \hat{n}_{i-1} + \hat{n}_{i+1}$ and $w_i = \varepsilon(1 - \hat{n}_i) + (1 - \varepsilon)\hat{n}_i$. As will become clear immediately it is useful to substitute the explicit form of f_i and, through a shift of the summation variable, rewrite the master operator as

$$W^{\text{FA}} = \sum_i W_i^{\text{FA}}, \quad W_i^{\text{FA}} = (F_{i+1} - 1)\hat{n}_i w_{i+1} + (F_i - 1)\hat{n}_{i+1} w_i. \quad (18)$$

The key feature of Eq. (18) is that W_i^{FA} operates only in the subspace $|n_i, n_{i+1}\rangle$. It therefore represents a *pair reaction process*. In the analysis of pair reaction processes it is conventional to choose an explicit representation for the basis $|0\rangle = \begin{pmatrix} 1 \\ 0 \end{pmatrix}$ and $|1\rangle = \begin{pmatrix} 0 \\ 1 \end{pmatrix}$. All operators then have appealingly simple matrix representations. From Eqs. (15) and (16) one has $\hat{n}_i = \begin{pmatrix} 0 & 0 \\ 0 & 1 \end{pmatrix}_i$ and $F_i = \begin{pmatrix} 0 & 1 \\ 1 & 0 \end{pmatrix}_i$. In particular, the FA master operator in the $|n_i, n_{i+1}\rangle$ subspace becomes

$$W_i^{\text{FA}} = \begin{pmatrix} 0 & 0 & 0 & 0 \\ 0 & -\beta & 0 & \gamma \\ 0 & 0 & -\beta & \gamma \\ 0 & \beta & \beta & -2\gamma \end{pmatrix}_{i, i+1}, \quad (19)$$

with $\beta = \varepsilon$ and $\gamma = 1 - \varepsilon$. The rows and columns of this matrix correspond to the configurations 00, 01, 10 and 11 from top to bottom and left to right, respectively. Consequently β is the branching rate, i.e. the rate for processes $01 \rightarrow 11$ and $10 \rightarrow 11$, while γ is the rate for coagulations $11 \rightarrow 01$ and $11 \rightarrow 10$.

We emphasize that the transitions $101 \rightarrow 111$ or $111 \rightarrow 101$ are accounted for correctly within this pair reaction description. In the case $101 \rightarrow 111$, for instance, one has $f_i(\mathbf{n}) = 2$ and $w_i(\mathbf{n}) = \varepsilon$ according to Eqs. (6) and (7), which amounts to a transition rate of 2ε . Equivalently, from Eqs. (18) and (19) the process $101 \rightarrow 111$ is

achieved by either branching to the right $\underline{101} \rightarrow \underline{111}$ or to the left $\underline{101} \rightarrow \underline{111}$ so that its total rate is again $\varepsilon + \varepsilon = 2\varepsilon$ as required. The pair reaction picture is of course exact.

We note that a modified version of the FA model with kinetic constraint $f_i(\mathbf{n}) = n_{i-1} + n_{i+1} - n_{i-1}n_{i+1}$ has often been used in the literature since it was first proposed [47]. It has certain advantages for simulations because $f_i \in \{0, 1\}$ is just a binary variable indicating whether the constraint of having at least one mobile neighbour is satisfied. However, for analytical work the presence of the quadratic term $n_{i-1}n_{i+1}$ is awkward and prevents in particular a pair reaction representation like the one above. Nevertheless the scaling behaviour in the modified FA model is expected to match with the original version [26] discussed here.

1.1. Effective Dynamics

The branching and coagulation process Eq. (19) gives rise to the remarkably rich dynamics of the FA model. Here we are interested in the evolution after a quench from a random uncorrelated initial state (equilibrium at $T = \infty$) to some low temperature $T \ll 1$ where $\varepsilon \sim e^{-1/T} \ll 1$. It is well known that the dynamics then evolves in distinct stages with separated time scales [27].

On the $\mathcal{O}(1)$ time scale activated states relax into blocked configurations. That is, the dynamics is controlled by coagulation processes $11 \rightarrow 01$ or 10 which proceed with rate $\gamma \sim 1$ until no further activated states 11 remain. This process has been analyzed in [48, 49]. The density of excitations drops from its initial value of $c_0 = \frac{1}{2}$ to $c_0 \exp(-c_0)$. Branching events like $10 \rightarrow 11$ only become relevant for times $t = \mathcal{O}(1/\varepsilon)$ since their rate is $\beta = \varepsilon \ll 1$. Such processes increase the energy $\mathcal{H} = \sum_i n_i$ and thus require thermal activation. The lifetime of the resulting activated state is $\mathcal{O}(1)$ because the excitations still coagulate with rate $\gamma \sim 1$, either back into the original state 10 or into 01 , each with equal probability. Due to this separation of time scales the probability to find an activated state at any given moment t is $\mathcal{O}(\varepsilon)$. At low temperatures $\varepsilon \ll 1$ branching events therefore effectively reduce to diffusion steps $01 \rightleftharpoons 10$, the rate of which is $d = \beta/2 = \varepsilon/2$. The FA dynamics on the $\mathcal{O}(1/\varepsilon)$ time scale is effectively that of diffusion and coagulation [32, 33, 34],

$$W_i^c = \begin{pmatrix} 0 & 0 & 0 & 0 \\ 0 & -d & d & \gamma \\ 0 & d & -d & \gamma \\ 0 & 0 & 0 & -2\gamma \end{pmatrix}_{i,i+1}. \quad (20)$$

This statement becomes exact in the limit $\varepsilon \rightarrow 0$ at fixed scaled time $\tilde{t} = \varepsilon t$. In other words, the evolution operators satisfy $\exp(W^{\text{FA}}\tilde{t}/\varepsilon) \sim \exp(W^c\tilde{t}/\varepsilon)$. In units of scaled time \tilde{t} the effective master operator $\tilde{W}^c = \varepsilon^{-1}W^c$ has diffusion rate $\tilde{d} = 1/2$ while the coagulation rate $\tilde{\gamma} \sim 1/\varepsilon \rightarrow \infty$ becomes formally infinite. (The process nevertheless remains well-defined because it is diffusion limited.)

At small but finite $\varepsilon \ll 1$ a third dynamical regime appears for times $t = \mathcal{O}(1/\varepsilon^2)$. Double-branching events $100 \rightarrow 110 \rightarrow 111$, which have rate $\mathcal{O}(\varepsilon^2)$, can then no longer

be neglected. Such triples relax with probability $1/2$ into 101 , so that two stable mobility excitations emerge. This process continuously generates new mobility excitations and thus counteracts the diffusion and coagulation dynamics discussed above. On a time scale of $\mathcal{O}(1/\varepsilon^2)$ or larger a crossover must therefore set in that eventually drives the FA model into equilibrium. A simple argument shows [27] that equilibrium is attained only for times of $\mathcal{O}(1/\varepsilon^3)$.

In our analysis of aging in the FA model we focus on the nonequilibrium regime of times $1 \ll t \ll 1/\varepsilon^2$ or more precisely scaled times $\tilde{t} = \varepsilon t = \mathcal{O}(1)$. In units of \tilde{t} the evolution is then governed by the diffusion and coagulation process Eq. (20) with rates $\tilde{d} = 1/2$ and $\tilde{\gamma} \sim 1/\varepsilon \gg 1$. We will concentrate in particular on the scaling that emerges for large \tilde{t} . At finite temperature $\varepsilon > 0$ this scaling refers to times $\tilde{t} \gg 1$ but still $\tilde{t} \ll 1/\varepsilon$ since Eq. (20) does not account for the onset of branching processes at $t = \mathcal{O}(1/\varepsilon^2)$. In other words, whenever we talk about asymptotic behaviour for $\tilde{t} \rightarrow \infty$ it is understood that the zero-temperature limit $\varepsilon \rightarrow 0$ is taken first.

We will later want to analyze response functions resulting from local perturbations $\delta\mathcal{H} = -\sum_i h_i n_i$. The impact of the latter on the effective dynamics Eq. (20) is easily derived. In the Glauber rates Eq. (6), which are defined through $w_i(\mathbf{n}) = [1 + \exp(\Delta_i \mathcal{H}/T)]^{-1}$ with $\Delta_i \mathcal{H}$ the change in energy caused by the flip, ε is then replaced by the local equilibrium excitation density

$$\varepsilon_i = \frac{1}{1 + e^{(1-h_i)/T}} \approx \varepsilon(1 + h_i/T), \quad (21)$$

to linear order in h_i . Consequently the branching rates from sites $i-1$ and $i+1$ to site i in the FA master operator Eq. (19) become $\beta = \varepsilon_i$; corresponding changes in the coagulation rates $\gamma = 1 + \mathcal{O}(\varepsilon)$ are negligible at low temperature. In the effective dynamics Eq. (20) on the $\mathcal{O}(1/\varepsilon)$ time scale we then have $d = \beta/2 = \varepsilon_i/2$ for diffusion from sites $i-1$ and $i+1$ to site i or, in scaled time \tilde{t} , $\tilde{d} \approx 1/2 + h_i/(2T)$ and $\tilde{\gamma} = \mathcal{O}(1/\varepsilon)$. In a linear response calculation on the $\tilde{t} = \mathcal{O}(1)$ time scale and at low temperature $\varepsilon \ll 1$, a field h_i thus enhances the rates for diffusion towards site i . Physically, this effect arises because diffusion in the FA model is an activated process.

2. A Useful Mapping

The effective DLPC dynamics of the FA model on the $\mathcal{O}(1/\varepsilon)$ time scale can be mapped onto a DLPA process. The latter admits an exact solution only for a special set of rates. We argue below that the scaling of certain observables, which includes in particular the domain size distribution, is robust under this modification of the rates. This will allow us to obtain various exact scaling results for the low temperature dynamics. We always focus on the $\mathcal{O}(1/\varepsilon)$ time scale; to simplify the notation we will drop all tildes from now on, effectively using $1/\varepsilon$ as the unit of time.

The equivalence of entire classes of diffusion limited reaction processes has been established in [42]. The effective DLPC dynamics, Eq. (20), of the FA model in particular

is equivalent to the process

$$W_i^a = \begin{pmatrix} 0 & 0 & 0 & \alpha \\ 0 & -d & d & 0 \\ 0 & d & -d & 0 \\ 0 & 0 & 0 & -\alpha \end{pmatrix}_{i,i+1}, \quad (22)$$

which describes diffusion limited pair annihilation. Here d is the rate for diffusion $10 \rightleftharpoons 01$, while α is the rate for pair annihilation $11 \rightarrow 00$. This result is established through a local stochastic similarity transformation with $b = |0\rangle\langle 0| + 2|1\rangle\langle 1| - |0\rangle\langle 1|$, or in matrix representation [43],

$$b = \begin{pmatrix} 1 & -1 \\ 0 & 2 \end{pmatrix} \quad \text{with} \quad b^{-1} = \begin{pmatrix} 1 & \frac{1}{2} \\ 0 & \frac{1}{2} \end{pmatrix}. \quad (23)$$

In terms of

$$B = b^{\otimes N} \quad \text{and} \quad B^{-1} = (b^{-1})^{\otimes N}, \quad (24)$$

one has

$$W^c = BW^aB^{-1}, \quad (25)$$

if W^c and W^a share the same diffusion rate d but $\alpha = 2\gamma$. This is readily proved: since the transformation is local and because $W^{c,a} = \sum_i W_i^{c,a}$ are pair reaction processes it is sufficient to consider the local master operators W_i^a and W_i^c in the $|n_i, n_{i+1}\rangle$ subspace. A simple matrix multiplication then shows that $W_i^c = (b \otimes b)W_i^a(b^{-1} \otimes b^{-1})$.

We note as an aside that there is in fact a direct mapping [34] that establishes the equivalence of the FA model and the DLPA process Eq. (22) on the $\mathcal{O}(1/\varepsilon)$ time scale, without having to proceed via the effective DLPC dynamics. The FA master operator Eq. (19) exactly maps onto DLPA, Eq. (22), but with an additional pair creation process $00 \rightarrow 11$ of rate $\mathcal{O}(\varepsilon^2)$. The latter is irrelevant for the dynamics on the $\mathcal{O}(1/\varepsilon)$ time scale so that we are once again left with the DLPA process Eq. (22).

Let us now consider how observables transform under the mapping B . The dynamics of a generic observable A in DLPC is given by

$$\langle A(t) \rangle_c = \langle e|A e^{W^c t}|P(0)\rangle. \quad (26)$$

By inserting identity operators BB^{-1} and via Eq. (25) this becomes

$$\langle A(t) \rangle_c = \langle e|B\tilde{A}e^{W^a t}B^{-1}|P(0)\rangle, \quad (27)$$

where $\tilde{A} = B^{-1}AB$. Note that $\langle e|B = [(\langle 0| + \langle 1|)b]^{\otimes N} = \langle e|$ according to Eqs. (12) and (23); likewise $\langle e|B^{-1} = \langle e|$. In order to eliminate B^{-1} in Eq. (27) an initial state $|P(0)\rangle$ must be specified. Consider the example of an uncorrelated and homogeneous initial state with particle density $0 < \rho \leq 1$,

$$|P(0)\rangle = |\rho\rangle = [(1-\rho)|0\rangle + \rho|1\rangle]^{\otimes N}. \quad (28)$$

Then $B^{-1}|\rho\rangle = [(1-\rho)b^{-1}|0\rangle + \rho b^{-1}|1\rangle]^{\otimes N} = [(1-\frac{1}{2}\rho)|0\rangle + \frac{1}{2}\rho|1\rangle]^{\otimes N} = |\frac{1}{2}\rho\rangle$ and

$$\langle A(t) \rangle_c = \langle e|A e^{W^c t}|\rho\rangle = \langle e|\tilde{A} e^{W^a t}|\frac{1}{2}\rho\rangle = \langle \tilde{A}(t) \rangle_a. \quad (29)$$

This equation states that the dynamics of an observable A in DLPC with initial density ρ is identical to that of \tilde{A} in DLPA for initial density $\rho/2$. One has to bear in mind, however, that \tilde{A} is generally a non-diagonal operator and so cannot be interpreted as a standard physical observable. Setting $A = \hat{n}$, for instance, yields

$$\tilde{n} = b^{-1}\hat{n}b = |0\rangle\langle 1| + |1\rangle\langle 1|. \quad (30)$$

The usefulness of Eq. (29) is preserved only by the fact that \tilde{A} is projected onto $\langle e|$. For the number operator ($\langle 0| + \langle 1|$) $\tilde{n} = 2\langle 1| = 2(\langle 0| + \langle 1|)\hat{n}$ as one easily verifies. More generally this implies [43]

$$\langle e|\hat{n}_{i_1}\hat{n}_{i_2}\dots\hat{n}_{i_m}e^{W^c t}|\rho\rangle = 2^m\langle e|\hat{n}_{i_1}\hat{n}_{i_2}\dots\hat{n}_{i_m}e^{W^{at}}|\frac{1}{2}\rho\rangle, \quad (31)$$

for ordered (and hence distinct) $i_1 < i_2 < \dots < i_m$. This relates equal-time particle correlations of arbitrary order in DLPC and DLPA in a simple manner. A more convenient set of observables for our purposes will be ($i_1 < i_2$)

$$E_{i_1, i_2} = \prod_{k=i_1}^{i_2-1} (1 - \hat{n}_k) \quad \text{and} \quad P_{i_1, i_2} = \prod_{k=i_1}^{i_2-1} (1 - 2\hat{n}_k), \quad (32)$$

which we refer to as empty and parity interval operators, respectively [50, 51]. This is for obvious reasons: $E_{i_1, i_2}|P(t)\rangle = |P(t)\rangle$ if the interval $\{i_1, i_1 + 1, \dots, i_2 - 1\}$ contains no particles, i.e. is empty, and $E_{i_1, i_2}|P(t)\rangle = 0$ otherwise. Similarly $P_{i_1, i_2}|P(t)\rangle = (-1)^m|P(t)\rangle$ measures the parity of the number of particles m contained in the same interval. From Eq. (29) one has the transformation law

$$\langle e|E_{i_1, i_2}\dots E_{i_{2k-1}, i_{2k}}e^{W^c t}|\rho\rangle = \langle e|P_{i_1, i_2}\dots P_{i_{2k-1}, i_{2k}}e^{W^{at}}|\frac{1}{2}\rho\rangle, \quad (33)$$

again assuming the $i_1 < i_2 < \dots < i_{2k}$ are ordered. This expression is of course equivalent to Eq. (31). But its physical meaning is more appealing: empty interval probabilities in DLPC directly map onto parity probabilities in DLPA if the initial state is adjusted appropriately.

The mapping establishes that equivalent to the effective DLPC dynamics of the FA model, Eq. (20), with rates $d = 1/2$ and $\gamma \sim 1/\varepsilon \gg 1$, is the DLPA process of Eq. (22) with rates $d = 1/2$ and $\alpha = 2\gamma \sim 2/\varepsilon \gg 1$. However, no exact solutions are known for either of these two processes. In DLPC the only exception is the process with identical diffusion and coagulation rates, $\gamma = d$, for which the master operator W^c admits a free fermion mapping [42]; obviously the same is true in the equivalent DLPA process with $\alpha = 2d$. In the following we analyze the dynamics of these particular free fermion DLPC and DLPA processes in more detail. Thereafter we discuss to what extent the results depend on reaction rates.

Exact results for reaction-diffusion problems are often related to integrable quantum spin chains [40]. Indeed, the most efficient way to generate explicit results for our free fermion DLPC and DLPA processes is to note that these are in turn equivalent to zero temperature dynamics of the Glauber Ising spin chain [52]. The latter is defined on a one-dimensional lattice $i = 1, 2, \dots, N$ of Ising spins $\sigma_i \in \{-1, +1\}$. The probability $p(\boldsymbol{\sigma}, t)$ for being in state $\boldsymbol{\sigma} = (\sigma_1, \sigma_2, \dots, \sigma_N)$ at time t is governed by a master equation

of the form Eq. (4) if one replaces \mathbf{n} by $\boldsymbol{\sigma}$. Likewise the transition rates are of the form Eq. (5) but without kinetic constraint, i.e. effectively $f_i(\boldsymbol{\sigma}) = 1$. The spin flip rates in the Glauber Ising model at $T = 0$ are $w_i(\boldsymbol{\sigma}) = \frac{1}{2}[1 - \frac{1}{2}\sigma_i(\sigma_{i-1} + \sigma_{i+1})]$ and represent nearest neighbour ferromagnetic interactions. A connection to DLPA is established by considering the defect or domain wall observables $n_i = \frac{1}{2}(1 - \sigma_i\sigma_{i+1}) \in \{0, 1\}$. Writing \uparrow and \downarrow for spin configurations $\sigma = +1$ and $\sigma = -1$, respectively, transitions $\uparrow\uparrow\downarrow \rightleftharpoons \uparrow\downarrow\downarrow$ then correspond to diffusion $01 \rightleftharpoons 10$ of the domain wall. The rate for this is $d = w_i(\boldsymbol{\sigma}) = \frac{1}{2}$. Similarly $\uparrow\downarrow\uparrow \rightarrow \uparrow\uparrow\uparrow$ translates into annihilation $11 \rightarrow 00$ of domain walls and has rate $\alpha = w_i(\boldsymbol{\sigma}) = 1$ (which satisfies the free fermion condition $\alpha = 2d$). The reverse process of pair creation $00 \rightarrow 11$ is not possible under zero temperature dynamics. Together, these arguments show that the spin dynamics in the Glauber Ising chain correspond to a DLPA process of the domain walls [53]. We now exploit this connection to extract results for DLPA. It is convenient to introduce an operator formalism analogous to Eqs. (8) - (14) by simply replacing the $|0\rangle, |1\rangle$ basis with the local spin basis $|\uparrow\rangle, |\downarrow\rangle$. Further denote by σ^z the spin operator $\sigma^z = |\uparrow\rangle\langle\uparrow| - |\downarrow\rangle\langle\downarrow|$ and by $W^\sigma = \sum_i (\sigma_i^x - 1) w_i$ the master operator of the Glauber Ising chain; here $\sigma_i^x = (|\uparrow\rangle\langle\downarrow| + |\downarrow\rangle\langle\uparrow|)_i$ plays the role of the flip operator Eq. (16). Using that the domain wall operator in the spin basis is $\hat{n}_i = \frac{1}{2}(1 - \sigma_i^z \sigma_{i+1}^z)$ the parity operator for the number of domain walls becomes

$$P_{i_1, i_2} = \prod_{k=i_1}^{i_2-1} (1 - 2\hat{n}_k) = \prod_{k=i_1}^{i_2-1} \sigma_k^z \sigma_{k+1}^z = \sigma_{i_1}^z \sigma_{i_2}^z, \quad (34)$$

since $(\sigma^z)^2 = 1$. This equation expresses the obvious fact that if σ_{i_1} and σ_{i_2} are aligned there must be an even number of sign-changes, i.e., domain walls, in the region between them. The fact that domain walls perform DLPA combined with Eq. (34) supplies us with the result

$$\langle e|P_{i_1, i_2} \dots P_{i_{2k-1}, i_{2k}} e^{W^{\text{a}t}} |\frac{1}{2}\rho\rangle = \langle e|\sigma_{i_1}^z \sigma_{i_2}^z \dots \sigma_{i_{2k}}^z e^{W^{\sigma t}} |P_\sigma(0)\rangle, \quad (35)$$

for $i_1 < i_2 < \dots < i_{2k}$ as usual. The dynamics of parity probabilities in the DLPA process with diffusion rate $d = 1/2$ and annihilation rate $\alpha = 1$ are identical to spin correlations in the zero temperature dynamics of the Glauber Ising chain. The initial state of the spin system $|P_\sigma(0)\rangle$ corresponding to the uncorrelated and homogeneous initial state $|\frac{1}{2}\rho\rangle$ in DLPA is determined by setting $t = 0$ in Eq. (35). Then $\langle e|P_{i_1, i_2} \dots P_{i_{2k-1}, i_{2k}} |\frac{1}{2}\rho\rangle = \langle e|P_{i_1, i_2} |\frac{1}{2}\rho\rangle \dots \langle e|P_{i_{2k-1}, i_{2k}} |\frac{1}{2}\rho\rangle$ and $\langle e|P_{i, j} |\frac{1}{2}\rho\rangle = (1 - \rho)^{j-i}$ factorizes completely since $|\frac{1}{2}\rho\rangle$ is uncorrelated and thus ‡

$$\langle e|\sigma_{i_1}^z \sigma_{i_2}^z \dots \sigma_{i_{2k}}^z |P_\sigma(0)\rangle = \prod_{\lambda=1}^k (1 - \rho)^{i_{2\lambda} - i_{2\lambda-1}}. \quad (36)$$

‡ Here the thermodynamic limit $N \rightarrow \infty$ was taken. In a finite system DLPA conserves the parity $P_{1, N}$ of the total particle number. The sectors of even and odd parity evolve independently and map onto Ising systems with periodic and antiperiodic boundary conditions, respectively. In the $N \rightarrow \infty$ limit the two sets of boundary conditions give identical results and so do not have to be distinguished.

These are precisely the equilibrium correlations, $|P_\sigma(0)\rangle = |P_{\text{eq}}(T_0)\rangle$, for the Ising Hamiltonian $\mathcal{H} = -J \sum_i \sigma_i \sigma_{i+1}$ at temperature T_0 if

$$\tanh(J/T_0) = 1 - \rho. \quad (37)$$

Altogether, from Eqs. (33) and (35), empty interval probabilities in the DLPC process with identical diffusion $d = 1/2$ and coagulation $\gamma = 1/2$ rates are thus given by

$$\langle e|E_{i_1, i_2} \dots E_{i_{2k-1}, i_{2k}} e^{W^c t} |\rho\rangle = \langle e|\sigma_{i_1}^z \sigma_{i_2}^z \dots \sigma_{i_{2k}}^z e^{W^{\sigma t}} |P_{\text{eq}}(T_0)\rangle, \quad (38)$$

where $i_1 < i_2 < \dots < i_{2k}$. Equation (38) is the central result of this section. It directly relates spin correlations in the Glauber Ising chain after a quench from temperature $T_0 > 0$ to $T = 0$ to the dynamics of (multi) empty interval observables in DLPC for initial density $0 < \rho \leq 1$. The required spin correlations appearing on the right hand side of Eq. (38) were derived in [54]. The simplest result is obtained for the initially filled state $\rho = 1$ which corresponds to $T_0 = \infty$ according to Eq. (37). One then has [54]

$$\langle e|E_{i_1, i_2} \dots E_{i_{2k-1}, i_{2k}} e^{W^c t} |1\rangle = \sum_{\pi \in \mathcal{P}(k)} (-1)^\pi \prod_{\lambda=1}^k H_{i_{\pi(2\lambda)} - i_{\pi(2\lambda-1)}}(2t). \quad (39)$$

Here $\pi : \{1, 2, \dots, 2k\} \mapsto \{1, 2, \dots, 2k\}$ denotes an index permutation, and $(-1)^\pi$ its sign; the sum runs over all permutations in the set $\mathcal{P}(k)$ of ordered pairings of the numbers $\{1, 2, \dots, 2k\}$. In an ordered pairing the entries are ordered within pairs, $\pi(1) < \pi(2)$, $\pi(3) < \pi(4)$, \dots , $\pi(2k-1) < \pi(2k)$, and the pairs are arranged in order of their first entry so that $\pi(1) < \pi(3) < \dots < \pi(2k-1)$. An expression for the function $H_n(t)$ is given in Eq. (A.8). We remark that Eq. (39) also applies in the case $\rho < 1$, i.e. $T_0 < \infty$, if one replaces H_n by the function H_n'' given in [54]. In subsequent sections we will repeatedly make use of the result Eq. (39) for the special cases $k = 1, 2$ where it reduces to

$$\langle e|E_{i_1, i_2} e^{W^c t} |1\rangle = H_{i_2 - i_1}(2t), \quad (40)$$

$$\langle e|E_{i_1, i_2} E_{i_3, i_4} e^{W^c t} |1\rangle = [H_{i_2 - i_1} H_{i_4 - i_3} - H_{i_3 - i_1} H_{i_4 - i_2} + H_{i_4 - i_1} H_{i_3 - i_2}](2t). \quad (41)$$

Both expressions, like Eq. (39), only apply for strictly ordered indices. In Eq. (41) we have introduced the short hand notation $[\cdot](x)$ to indicate that all functions enclosed in the square brackets have the same argument x .

2.1. Domain Size Distribution

At this point we have the exact result Eq. (39) for empty interval densities in the free fermion DLPC process, with rates $d = \gamma = 1/2$. However, we are actually interested in the effective FA process which has the correct diffusion rate $d = 1/2$ but a much larger coagulation rate $\gamma \sim 1/\varepsilon \gg 1$. In order to understand how the latter affects the dynamics of DLPC it is instructive to consider the domain size distribution. Using spatial homogeneity we define the density of domains of size $k = j - i \geq 1$ as

$$D_{j-i}(t) = \langle e|\hat{n}_i(1 - \hat{n}_{i+1}) \dots (1 - \hat{n}_{j-1})\hat{n}_j e^{W^c t} |1\rangle. \quad (42)$$

Equivalently $D_{j-i}(t) = \langle e | (E_{i+1,j} - E_{i,j} - E_{i+1,j+1} + E_{i,j+1}) e^{Wc_t} | 1 \rangle$ as follows by re-writing $\hat{n}_i = 1 - (1 - \hat{n}_i)$ and similarly for \hat{n}_j . In the free fermion case these empty interval densities are given by Eq. (40) so that $D_k(t) = [H_{k-1} - 2H_k + H_{k+1}](2t)$. Applying the recursion Eq. (A.9) turns this expression into

$$D_k(t) = e^{-2t}[I_{k-1} - I_{k+1}](2t), \quad (43)$$

where the $I_n(t)$ are modified Bessel functions, see Eq. (A.2). This remarkably simple exact result is well known [55]. Since one particle may be associated with each domain the exact particle concentration $c(t) = \langle \hat{n}_i(t) \rangle$ follows by summing this over k . The sum is telescopic and hence

$$c(t) = \sum_{k=1}^{\infty} D_k(t) = e^{-2t}[I_0 + I_1](2t). \quad (44)$$

Obviously the results Eqs. (43) and (44) apply exactly only for the free fermion ($d = \gamma = 1/2$) DLPC process with initial density $\rho = 1$. However, it is known that both the concentration and the domain size distribution have remarkably robust scalings [56]. From Eq. (44) and the asymptotic expansion Eq. (A.6) the concentration scales like $c(t) \sim 1/\sqrt{\pi t}$ for $t \rightarrow \infty$. This leading order result applies in fact to any DLPC process with $d = 1/2$ and arbitrary $\gamma > 0$ and regardless of the initial density $\rho > 0$ [56]. To understand why, consider the scaling of the domain size distribution Eq. (43). In the limit $t \rightarrow \infty$ and for domain sizes $k = \mathcal{O}(\sqrt{t})$ one finds, via Eqs. (A.4) and (A.7), the scaling

$$D_k(t) = \frac{k}{t} e^{-2t} I_k(2t) \sim \frac{1}{\sqrt{\pi t}} \frac{k}{2\sqrt{t}} e^{-k^2/(4t)}. \quad (45)$$

Typical domains have a size of $k = \mathcal{O}(\sqrt{t})$ and density $\mathcal{O}(t^{-1})$. Integrating Eq. (45) over $\kappa = k/(2\sqrt{t}) \in]0, \infty[$ shows that only typical domains of length $k = \mathcal{O}(\sqrt{t})$ contribute to the scaling $c(t) \sim 1/\sqrt{\pi t}$. Large domains $k \gg \sqrt{t}$ are exponentially unlikely and also small domains $k \ll \sqrt{t}$ are of subdominant density. In fact, the density of finite domains with $k = \mathcal{O}(1)$ is $D_k(t) \sim k/(2\sqrt{\pi} t^{3/2}) = \mathcal{O}(t^{-3/2})$, while for typical domains $D_k(t) = \mathcal{O}(t^{-1})$. The scaling of DLPC is thus controlled by typical domains. For such domains to disappear, the delimiting particles first have to diffuse for a time $\mathcal{O}(t)$ before there is a significant chance that they will occupy adjacent sites. The coagulation reaction itself then occurs on an $\mathcal{O}(1)$ time scale for any $\gamma > 0$. It therefore only has a subdominant effect on the rate at which typical domains disappear, and the process is said to be in the diffusion controlled regime [56]. The scaling for the density of typical domains Eq. (45) thus applies to any DLPC process with $d = 1/2$ and $\gamma > 0$, and regardless of the initial density $\rho > 0$. The precise value of the coagulation rate γ only shows up in the coefficient for the density of small domains $k = \mathcal{O}(1)$ which, in any case, is $\mathcal{O}(t^{-3/2})$.

The above discussion illustrates that the initial density ρ as well as the coagulation rate γ only have a subdominant effect on the evolution of DLPC [56] for $t \gg 1$; recall that in the FA model this long-time regime corresponds to unscaled times much larger

than $1/\varepsilon$ but much smaller $1/\varepsilon^2$. The long-time behaviour of the effective FA process Eq. (20) can therefore be extracted from the analytically tractable free fermion case ($d = \gamma = 1/2$). We also exploit the irrelevance of the initial density for the leading order long-time results to set $\rho = 1$; this simplifies the mathematics and produces differences to the case $\rho < 1$ only in subdominant terms.

Note that the above simplifications will hold for all observables except for those which show particular sensitivity to the density of small domains; we will return to this point in our discussion of response functions.

3. Two-Time Quantities

In the following we derive exact scaling expressions for the two-time correlation and response functions of the FA model in the long-time regime discussed above, by exploiting the equivalence to the free fermion DLPC process with initial density $\rho = 1$.

The mapping from DLPC to DLPA, which is our key for deriving results, cannot be applied in a practical way to multi-time quantities. Consider, for instance,

$$\langle A_1(t)A_2(t_w) \rangle_c = \langle e|A_1 e^{W^c \Delta t} A_2 e^{W^c t_w} |\rho \rangle, \quad (46)$$

where t_w is the waiting time since preparation of the system and $\Delta t = t - t_w$ is the time interval to the later measurement at time t . Inserting identity operators BB^{-1} yields $\langle e|\tilde{A}_1 e^{W^a \Delta t} \tilde{A}_2 e^{W^a t_w} |\frac{1}{2}\rho \rangle$. But as discussed below Eq. (29) the mapped observables $\tilde{A}_{1,2} = B^{-1}A_{1,2}B$ are generally non-diagonal operators. While the projection $\langle e|\tilde{A}_1$ may reduce \tilde{A}_1 to a physical observable this is no longer the case for \tilde{A}_2 which is sandwiched between evolution operators.

We now demonstrate how the mapping can nevertheless be applied to multi-time quantities and in a physically sensible manner if the evolution operator is known. The discussion will proceed in the reverse order of Sec. 2: we first consider spin dynamics in the Glauber Ising chain, relate these to parity intervals in DLPA and then map onto DLPC. We exploit the following general result for the evolution of two-spin correlations $F_{\mathbf{i}}^{(2)}(t) = \langle e|\sigma_{i_1}^z \sigma_{i_2}^z e^{W^{\sigma} t} |\psi \rangle$ in the Glauber Ising model at zero temperature: in the notation of [54],

$$F_{\mathbf{i}}^{(2)}(t) = \sum_{j_1 < j_2} G_{\mathbf{i}, \mathbf{j}}^{(2)}(t) A_{\mathbf{j}}^{(2)} + H_{i_2 - i_1}(2t) A^{(0)}, \quad (47)$$

where

$$G_{\mathbf{i}, \mathbf{j}}^{(2)}(t) = e^{-2t} [I_{i_1 - j_1} I_{i_2 - j_2} - I_{i_1 - j_2} I_{i_2 - j_1}](t). \quad (48)$$

and the $A_{\mathbf{j}}^{(2)} = \langle e|\sigma_{j_1}^z \sigma_{j_2}^z |\psi \rangle$ are the correlations at time 0 while $A^{(0)} = \langle e|\psi \rangle$. Eq. (47) expresses a two-spin correlation at time t in terms of those in the general state $|\psi \rangle$ at $t = 0$. The corresponding two-spin Green's function $G_{\mathbf{i}, \mathbf{j}}^{(2)}(t)$ is expressed in Eq. (48) in terms of modified Bessel functions $I_n(t)$. The definition of the latter is recalled in Eq. (A.2), while $H_n(t)$ is stated explicitly in Eq. (A.8). Equation (47) applies for $i_1 < i_2$ and it is our convention throughout that sums as in Eq. (47) are taken over ordered

integer pairs $\mathbf{j} = (j_1, j_2)$. Now, given that Eq. (47) applies for arbitrary initial states $|\psi\rangle$ we may equivalently write

$$\langle e | \sigma_{i_1}^z \sigma_{i_2}^z e^{W^{\sigma t}} = \sum_{j_1 < j_2} G_{\mathbf{i}, \mathbf{j}}^{(2)}(t) \langle e | \sigma_{j_1}^z \sigma_{j_2}^z + H_{i_2 - i_1}(2t) \langle e |. \quad (49)$$

We refer to this object as the two-spin propagator; more general multi-spin propagators follow likewise from the general result given in [54]. Equation (49) has a direct analogue in DLPA. Recall that according to Eq. (34) the operator $\sigma_{i_1}^z \sigma_{i_2}^z = P_{i_1, i_2}$ measures the parity of the number of domain walls between sites i_1 and i_2 . This, combined with the fact that Glauber dynamics of the spin system correspond to DLPA of the domain walls, implies

$$\langle e | P_{\mathbf{i}} e^{W^{\sigma t}} = \sum_{j_1 < j_2} G_{\mathbf{i}, \mathbf{j}}^{(2)}(t) \langle e | P_{\mathbf{j}} + H_{i_2 - i_1}(2t) \langle e |, \quad (50)$$

which is the parity propagator in DLPA. A mapping to DLPC is now straightforward. Multiplying by B^{-1} from the right and inserting identity operators $B^{-1}B$ immediately yields the empty interval propagator in DLPC,

$$\langle e | E_{\mathbf{i}} e^{W^{\sigma t}} = \sum_{j_1 < j_2} G_{\mathbf{i}, \mathbf{j}}^{(2)}(t) \langle e | E_{\mathbf{j}} + H_{i_2 - i_1}(2t) \langle e |. \quad (51)$$

The expressions Eqs. (49–51) are rather remarkable. They show that propagating a two-spin operator forward in time in the Glauber Ising chain is equivalent to propagating a parity operator in DLPA or an empty interval operator in DLPC. Nevertheless, as we will see, the two-time quantities that follow from Eqs. (50) and (51) are not related in a simple way. Note also that in contrast to Eq. (46) no non-diagonal operators arise explicitly when the mapping is written in terms of the propagators: since Eqs. (50) and (51) are explicit representations of the evolution operator, a projection state $\langle e |$ is always available to absorb contributions from off-diagonal components of mapped operators. We finally add that via the identity Eq. (A.12) each of the above propagators can be reexpressed in a somewhat different but equivalent form, for instance

$$\langle e | E_{\mathbf{i}} e^{W^{\sigma t}} = \langle e | + \sum_{j_1 < j_2} G_{\mathbf{i}, \mathbf{j}}^{(2)}(t) \langle e | (E_{\mathbf{j}} - 1). \quad (52)$$

3.1. Two-Time Correlations

Using the DLPC propagator derived above we can now analyse the connected two-time correlation functions of mobility excitations (or defects) in the FA model,

$$C_{i-j}(t, t_w) = \langle e | \hat{n}_i e^{W^{\sigma} \Delta t} \hat{n}_j e^{W^{\sigma} t_w} | 1 \rangle - \langle e | \hat{n}_i e^{W^{\sigma} t} | 1 \rangle \langle e | \hat{n}_j e^{W^{\sigma} t_w} | 1 \rangle. \quad (53)$$

To understand nonequilibrium fluctuation-dissipation relations one also requires the associated response functions; these will be considered in the next subsection. It is useful to introduce the more general correlator

$$C_{\mathbf{i}, \mathbf{j}}(t, t_w) = \langle e | E_{\mathbf{i}} e^{W^{\sigma} \Delta t} E_{\mathbf{j}} e^{W^{\sigma} t_w} | 1 \rangle - \langle e | E_{\mathbf{i}} e^{W^{\sigma} t} | 1 \rangle \langle e | E_{\mathbf{j}} e^{W^{\sigma} t_w} | 1 \rangle, \quad (54)$$

which reduces to $C_{i-j}(t, t_w)$ for $\mathbf{i} = (i, i+1)$ and $\mathbf{j} = (j, j+1)$ since $\hat{n}_i = 1 - E_{i,i+1}$. The first step in evaluating Eq. (54) consists in decomposing the evolution operator $e^{W^c t} = e^{W^c \Delta t} e^{W^c t_w}$ and substituting the empty interval propagator Eq. (52) for both occurrences of $\langle e|E_{\mathbf{i}} e^{W^c \Delta t}$ in Eq. (54). Simplifications occur due to probability conservation, $\langle e|e^{W^c \Delta t} = \langle e|$, and the normalization $\langle e|1\rangle = 1$ of the initial state, giving

$$C_{\mathbf{i}, \mathbf{j}}(t, t_w) = \sum_{k_1 < k_2} G_{\mathbf{i}, \mathbf{k}}^{(2)}(\Delta t) (\langle e|E_{\mathbf{k}} E_{\mathbf{j}} e^{W^c t_w}|1\rangle - \langle e|E_{\mathbf{k}} e^{W^c t_w}|1\rangle \langle e|E_{\mathbf{j}} e^{W^c t_w}|1\rangle). \quad (55)$$

The connected two-time empty interval correlations are now reduced to connected one-time averages. We remark that precisely the same expression applies in DLPA if one replaces the empty by parity interval operators. Nevertheless, as indicated above, the resulting two-time correlations are different. This is for the following reason: the sum in Eq. (55) runs over all ordered index pairs \mathbf{k} and thus there are inevitably overlaps of $E_{\mathbf{k}}$ with $E_{\mathbf{j}}$. In such cases the empty interval operators merge since $(1 - \hat{n}_i)^2 = 1 - \hat{n}_i$. Parity interval operators, on the other hand, cancel each other in regions of overlap because $(1 - 2\hat{n}_i)^2 = 1$. Differences in two-time correlations between DLPC and DLPA therefore arise due to the different reduction properties of empty and parity interval operators. For the case of empty intervals that we are interested in here one has

$$E_{k_1, k_2} E_{j_1, j_2} = \begin{cases} E_{k_1, k_2} E_{j_1, j_2} & k_1 < k_2 < j_1 < j_2 \\ E_{k_1, j_2} & k_1 < j_1 \leq k_2 \leq j_2 \\ E_{k_1, k_2} & k_1 < j_1 < j_2 < k_2 \\ E_{j_1, j_2} & j_1 \leq k_1 < k_2 \leq j_2 \\ E_{j_1, k_2} & j_1 \leq k_1 \leq j_2 < k_2 \\ E_{j_1, j_2} E_{k_1, k_2} & j_1 < j_2 < k_1 < k_2 \end{cases} \quad \text{for} \quad (56)$$

To proceed with the derivation of $C_{\mathbf{i}, \mathbf{j}}(t, t_w)$ the summation in Eq. (55) over the pair-correlation term must be broken up according to Eq. (56), with corresponding reductions in each sector. For the remaining averages, which are now of the form $\langle e|E_{l_1, l_2} e^{W^c t_w}|1\rangle$ and $\langle e|E_{l_1, l_2} E_{l_3, l_4} e^{W^c t_w}|1\rangle$ with strictly ordered indices $l_1 < l_2 < l_3 < l_4$, we substitute the results Eqs. (40) and (41) from above. At this point one has a rather bulky expression for $C_{\mathbf{i}, \mathbf{j}}(t, t_w)$. To simplify matters we focus on $\mathbf{j} = (j, j+1)$ – the case of interest – which narrows down several summation ranges, c.f. Eq. (56). It is then a tedious but trivial task to show that the various sums can be regrouped into the compact form

$$\begin{aligned} C_{\mathbf{i}, (j, j+1)}(t, t_w) &= [1 - H_1(2t_w)] \sum_{k_1 \leq j} \sum_{k_2 > j} G_{\mathbf{i}, \mathbf{k}}^{(2)}(\Delta t) H_{k_2 - k_1}(2t_w) \\ &+ \sum_{k_1 \leq j} \sum_{k_2 \leq j} G_{\mathbf{i}, \mathbf{k}}^{(2)}(\Delta t) H_{j+1 - k_1}(2t_w) [\delta_{k_2, j} + H_{j - k_2}(2t_w)] \\ &+ \sum_{k_1 > j} \sum_{k_2 > j} G_{\mathbf{i}, \mathbf{k}}^{(2)}(\Delta t) H_{k_2 - j}(2t_w) [\delta_{k_1, j+1} + H_{k_1 - j - 1}(2t_w)]. \end{aligned} \quad (57)$$

Here antisymmetry of $G_{\mathbf{i}, \mathbf{k}}^{(2)}(\Delta t)$ under permutation of $k_1 \leftrightarrow k_2$ and $H_0(2t_w) = 0$ was used. Finally we set $\mathbf{i} = (i, i+1)$ and rearrange Eq. (57) as follows: in each line the summation variables are changed from k_1, k_2 to $p, q \geq 0$ and the indices of the Green's

functions are simplified based on translational $G_{\mathbf{i},\mathbf{k}}^{(2)}(\Delta t) = G_{\mathbf{i}+\mathbf{l},\mathbf{k}+\mathbf{l}}^{(2)}(\Delta t)$ and reflection $G_{\mathbf{i},\mathbf{k}}^{(2)}(\Delta t) = G_{-\mathbf{i},-\mathbf{k}}^{(2)}(\Delta t)$ symmetry. In terms of $n = i - j$ the last two lines of Eq. (57) thereby become

$$\sum_{p,q=0}^{\infty} G_{(\pm n, \pm n-1), (p,q)}^{(2)}(\Delta t) H_{p+1}(2t_w) [\delta_{q,0} + H_q(2t_w)], \quad (58)$$

where the two signs $+n$ and $-n$ correspond to the third and second line of Eq. (57), respectively. For later convenience we point out that hidden in this expression lies a leading order cancellation in the limit of large t_w . Using that the Green's function in Eq. (58) changes sign when p and q are interchanged we can write

$$\sum_{p,q=0}^{\infty} G_{(\pm n, \pm n-1), (p,q)}^{(2)}(\Delta t) [\delta_{p,0} + H_p(2t_w)] [\delta_{q,0} + H_q(2t_w)] = 0. \quad (59)$$

Subtracting this vanishing expression from Eq. (58) replaces $H_{p+1}(2t_w)$ with $H_{p+1}(2t_w) - \delta_{p,0} - H_p(2t_w) = -e^{-2t_w} [I_p + I_{p+1}](2t_w)$, see Eq. (A.9). Similarly, in the first line of Eq. (57) we have $1 - H_1(2t_w) = e^{-2t_w} [I_0 + I_1](2t_w)$. Altogether our result for the connected two-time mobility correlation function defined in Eq. (53) becomes

$$\begin{aligned} C_n(t, t_w) &= e^{-2t_w} [I_0 + I_1](2t_w) \sum_{p,q=0}^{\infty} G_{(n,n+1), (-p,q+1)}^{(2)}(\Delta t) H_{p+q+1}(2t_w) \\ &\quad - \sum_{p,q=0}^{\infty} G_{(+n,+n-1), (p,q)}^{(2)}(\Delta t) e^{-2t_w} [I_p + I_{p+1}](2t_w) [\delta_{q,0} + H_q(2t_w)] \\ &\quad - \sum_{p,q=0}^{\infty} G_{(-n,-n-1), (p,q)}^{(2)}(\Delta t) e^{-2t_w} [I_p + I_{p+1}](2t_w) [\delta_{q,0} + H_q(2t_w)]. \end{aligned} \quad (60)$$

This expression is exact for free-fermion DLPC with unit initial density, but as argued above its scaling behaviour at large t_w applies to DLPC processes with arbitrary coagulation rate and initial density. This includes in particular the effective FA dynamics we are interested in. Equation (60) forms the basis for our subsequent discussion; the leading order cancellation with respect to t_w having been eliminated, it is well suited for long-time expansions.

3.2. Two-Time Response Functions

We now turn to the two-time response function conjugate to the two-time correlation $C_n(t, t_w)$ discussed above, which is given by

$$R_{i-j}(t, t_w) = \langle e | \hat{n}_i e^{W^c \Delta t} V_j e^{W^c t_w} | 1 \rangle, \quad (61)$$

where the operator $V_j = T [\partial W^c(h) / \partial h] |_{h=0}$ accounts for the perturbation $\delta \mathcal{H} = -h \hat{n}_j$ of the effective dynamics at t_w . Note that the response contains a factor of T consistent with our definition Eq. (2). By analogy to the correlations it is convenient to consider the more general response

$$R_{\mathbf{i},j}(t, t_w) = -\langle e | E_{\mathbf{i}} e^{W^c \Delta t} V_j e^{W^c t_w} | 1 \rangle, \quad (62)$$

which reduces to Eq. (61) for $\mathbf{i} = (i, i + 1)$ as is obvious from $E_{i,i+1} = 1 - \hat{n}_i$ and probability conservation $\langle e|e^{W^c \Delta t} V_j = \langle e|V_j = 0$. As before, substitution of the empty interval propagator Eq. (52) reduces the two-time average in Eq. (62) to a one-time average, which is most conveniently expressed in the form

$$R_{\mathbf{i},j}(t, t_w) = \sum_{k_1 < k_2} G_{\mathbf{i},\mathbf{k}}^{(2)}(\Delta t) R_{\mathbf{k},j}(t_w, t_w), \quad (63)$$

with the instantaneous response

$$R_{\mathbf{i},j}(t_w, t_w) = -\langle e|E_{\mathbf{i}} V_j e^{W^c t_w} |1\rangle. \quad (64)$$

In what follows we will first concentrate on the instantaneous response; from this the two-time response $R_{\mathbf{i},j}(t, t_w)$ then follows immediately via Eq. (63). The effect of the perturbation encoded in V_j has the explicit form

$$V_j = \frac{1}{2}(F_{j-1}F_j - 1)\hat{n}_{j-1}(1 - \hat{n}_j) + \frac{1}{2}(F_{j+1}F_j - 1)\hat{n}_{j+1}(1 - \hat{n}_j). \quad (65)$$

Here the first term is nonzero only if site j is empty and site $j - 1$ occupied, reflecting the increased rate for diffusion from $j - 1$ to j as discussed at the end of Sec. 1.1; the second term similarly captures the increased diffusion from $j + 1$ to j . It will become clear below that a decomposition of V_j into an asymmetric and symmetric contribution, $V_j = V_j^{(a)} + V_j^{(s)}$, is very useful:

$$V_j^{(a)} = \frac{1}{4}(F_{j-1}F_j - 1)(\hat{n}_{j-1} - \hat{n}_j) + \frac{1}{4}(F_{j+1}F_j - 1)(\hat{n}_{j+1} - \hat{n}_j), \quad (66)$$

$$V_j^{(s)} = \frac{1}{4}(F_{j-1}F_j - 1)(\hat{n}_{j-1} - \hat{n}_j)^2 + \frac{1}{4}(F_{j+1}F_j - 1)(\hat{n}_{j+1} - \hat{n}_j)^2. \quad (67)$$

The operator $V_j^{(a)}$ represents increased local diffusion rates $j - 1 \rightarrow j \leftarrow j + 1$ for entering site j but decreased ones for leaving it $j - 1 \leftarrow j \rightarrow j + 1$, thus $V_j^{(a)}$ *traps diffusing defects* at site j . Its symmetric counter-part $V_j^{(s)}$, on the other hand, corresponds to increased local diffusion rates between sites $j - 1 \rightleftharpoons j \rightleftharpoons j + 1$ in both directions and hence *speeds up the local dynamics*. Accordingly, the defect response function in the FA model may be decomposed into the contributions

$$R_n(t, t_w) = R_n^{(a)}(t, t_w) + R_n^{(s)}(t, t_w). \quad (68)$$

3.2.1. Asymmetric Perturbation We first discuss the effect of the asymmetric part of the perturbation. From Eq. (64) the corresponding instantaneous response function is

$$R_{\mathbf{i},j}^{(a)}(t_w, t_w) = -\langle e|E_{\mathbf{i}} V_j^{(a)} e^{W^c t_w} |1\rangle. \quad (69)$$

If $V_j^{(a)}$ acts entirely inside or outside of $E_{\mathbf{i}}$, then the instantaneous response vanishes: the empty interval density $\langle e|E_{\mathbf{i}} e^{W^c t_w} |1\rangle$ is only affected by the perturbation when applied at either boundary of $E_{\mathbf{i}}$, increasing/decreasing the rate for defects to enter/exit the interval. Substituting the expressions (32) and (66) for $E_{\mathbf{i}}$ and $V_j^{(a)}$, respectively, and using the commutation relation $(1 - \hat{n}_i)F_i = F_i\hat{n}_i$ one shows that

$$\begin{aligned} R_{\mathbf{i},j}^{(a)}(t_w, t_w) &= \frac{1}{4}(\delta_{j,i_1} - \delta_{j,i_1-1}) \langle e|(\hat{n}_{i_1-1} - \hat{n}_{i_1})^2 E_{i_1+1,i_2} e^{W^c t_w} |1\rangle \\ &\quad - \frac{1}{4}(\delta_{j,i_2} - \delta_{j,i_2-1}) \langle e|E_{i_1,i_2-1} (\hat{n}_{i_2-1} - \hat{n}_{i_2})^2 e^{W^c t_w} |1\rangle. \end{aligned} \quad (70)$$

This makes perfect sense: the Kronecker deltas enforce that j must be a relevant site and also carry the sign of the response, while the averages give its magnitude. In the first line, for instance, only the configurations $0_{i_1-1}1_{i_1}0_{i_1+1}\dots 0_{i_2-1}$ and $1_{i_1-1}0_{i_1}0_{i_1+1}\dots 0_{i_2-1}$ contribute, since these are susceptible to perturbations of the local diffusion rates between sites $i_1 - 1$ and i_1 and affect the empty interval observable E_i . To evaluate the averages it is convenient to rewrite $(\hat{n}_{i_1-1} - \hat{n}_{i_1})^2 = \hat{n}_{i_1-1}(1 - \hat{n}_{i_1}) + \hat{n}_{i_1} - \hat{n}_{i_1-1}\hat{n}_{i_1}$ whereby

$$(\hat{n}_{i_1-1} - \hat{n}_{i_1})^2 E_{i_1+1,i_2} = \hat{n}_{i_1-1}E_{i_1,i_2} + \hat{n}_{i_1}E_{i_1+1,i_2} - \hat{n}_{i_1-1}\hat{n}_{i_1}E_{i_1+1,i_2}. \quad (71)$$

The first two terms on the right hand side of this equation are related to the density of domains: the observable $\hat{n}_{i_1}E_{i_1+1,i_2}$, for instance, measures the density of domains $1_{i_1}0_{i_1+1}\dots 0_{i_1+n-1}1_{i_1+n}$ of any size $n \geq i_2 - i_1$ and hence

$$\langle e|\hat{n}_{i_1}E_{i_1+1,i_2} e^{W^c t_w}|1\rangle = \sum_{k=0}^{\infty} D_{i_2-i_1+k}(t_w). \quad (72)$$

Altogether we may rewrite Eq. (70) in the form

$$R_{i,j}^{(a)}(t_w, t_w) = \frac{1}{4}A_{i,j} \left[D_{i_2-i_1}(t_w) + 2 \sum_{k=1}^{\infty} D_{i_2-i_1+k}(t_w) \right] + \Delta_{i,j}^{(a)}(t_w, t_w), \quad (73)$$

where $A_{i,j} = \delta_{j,i_1} - \delta_{j,i_1-1} - \delta_{j,i_2} + \delta_{j,i_2-1}$ and

$$\begin{aligned} \Delta_{i,j}^{(a)}(t_w, t_w) &= -\frac{1}{4}(\delta_{j,i_1} - \delta_{j,i_1-1}) \langle e|\hat{n}_{i_1-1}\hat{n}_{i_1}E_{i_1+1,i_2} e^{W^c t_w}|1\rangle \\ &\quad + \frac{1}{4}(\delta_{j,i_2} - \delta_{j,i_2-1}) \langle e|E_{i_1,i_2-1}\hat{n}_{i_2-1}\hat{n}_{i_2} e^{W^c t_w}|1\rangle. \end{aligned} \quad (74)$$

The function $\Delta_{i,j}^{(a)}(t_w, t_w)$ in Eq. (73) was isolated since it is subdominant at large t_w and thus unimportant for the long-time scaling. The remaining terms on the r.h.s. of Eq. (73) contain a sum over the density of domains $D_n(t_w)$ which picks up its main contributions from domains of size $n = \mathcal{O}(\sqrt{t_w})$. In this regime $D_n(t_w)$ has a robust scaling form Eq. (45) that is independent of the coagulation rate and the same therefore applies to the leading long-time behaviour of the instantaneous asymmetric response. It is clear from Eq. (71) that $\Delta_{i,j}^{(a)}(t_w, t_w)$ corrects for the fact that, e.g., the configuration $1_{i_1-1}1_{i_1}0_{i_1+1}\dots 0_{i_2-1}$ does not respond to perturbations of the local diffusion rates between sites $i_1 - 1$ and i_1 . At long times such states with neighbouring defects have subdominant density in DLPC compared to states with isolated defects, and this is the intuitive reason why $\Delta_{i,j}^{(a)}(t_w, t_w)$, whose scaling does depend on the precise coagulation rate, is subdominant compared to the leading term in Eq. (73). (In the effective FA dynamics the probability of states containing adjacent defects is further suppressed by the fact that coagulation is essentially instantaneous.) Further discussion of $\Delta_{i,j}^{(a)}(t_w, t_w)$ may be found in Appendix B; here we focus on Eq. (73) which controls the asymptotic long-time scaling. Substituting the DLPC result Eq. (43) for $D_n(t_w)$ produces a telescopic sum in Eq. (73) and gives

$$R_{i,j}^{(a)}(t_w, t_w) = \frac{1}{4}A_{i,j} e^{-2t_w} [I_{i_2-i_1-1} + 2I_{i_2-i_1} + I_{i_2-i_1+1}](2t_w) + \Delta_{i,j}^{(a)}(t_w, t_w). \quad (75)$$

The associated two-time response function is readily obtained via Eq. (63). The ordered double sum over $k_1 < k_2$ reduces to semi-infinite ones due to $A_{i,j}$ but the latter may be recombined into full summations over all integers and evaluated using the convolution property Eq. (A.5). The resulting expression for the asymmetric part of the two-time response function Eq. (61) with $n = i - j$ is most compactly expressed as

$$R_n^{(a)}(t, t_w) = \partial_{t_w} \frac{1}{2} e^{-2t} I_n(t - t_w) [I_{n-1} + 2I_n + I_{n+1}](t + t_w) + \Delta_n^{(a)}(t, t_w). \quad (76)$$

3.2.2. Symmetric Perturbation The derivation of the response to a symmetric perturbation is largely analogous to the asymmetric case discussed above. We define

$$R_{i,j}^{(s)}(t_w, t_w) = -\langle e | E_i V_j^{(s)} e^{W^c t_w} | 1 \rangle. \quad (77)$$

Again a non-zero response occurs only if the perturbation is applied at either boundary of the empty interval E_i . Specifically one finds

$$R_{i,j}^{(s)}(t_w, t_w) = \frac{1}{4} (\delta_{j,i_1} + \delta_{j,i_1-1}) \langle e | (\hat{n}_{i_1-1} - \hat{n}_{i_1}) E_{i_1+1,i_2} e^{W^c t_w} | 1 \rangle \\ + \frac{1}{4} (\delta_{j,i_2} + \delta_{j,i_2-1}) \langle e | E_{i_1,i_2-1} (\hat{n}_{i_2-1} - \hat{n}_{i_2}) e^{W^c t_w} | 1 \rangle, \quad (78)$$

which is the symmetric counterpart to Eq. (70). This time we rewrite $\hat{n}_{i_1-1} - \hat{n}_{i_1} = \hat{n}_{i_1-1} (1 - \hat{n}_{i_1}) - \hat{n}_{i_1} + \hat{n}_{i_1-1} \hat{n}_{i_1}$ so that

$$(\hat{n}_{i_1-1} - \hat{n}_{i_1}) E_{i_1+1,i_2} = \hat{n}_{i_1-1} E_{i_1,i_2} - \hat{n}_{i_1} E_{i_1+1,i_2} + \hat{n}_{i_1-1} \hat{n}_{i_1} E_{i_1+1,i_2}, \quad (79)$$

and once more use Eq. (72) to express the averages $\langle e | \hat{n}_{i_1} E_{i_1+1,i_2} e^{W^c t_w} | 1 \rangle$ etc. in terms of domain densities $D_n(t_w)$. One finds

$$R_{i,j}^{(s)}(t_w, t_w) = -\frac{1}{4} B_{i,j} D_{i_2-i_1}(t_w) + \Delta_{i,j}^{(s)}(t_w, t_w), \quad (80)$$

where $B_{i,j} = \delta_{j,i_1} + \delta_{j,i_1-1} + \delta_{j,i_2} + \delta_{j,i_2-1}$ and

$$\Delta_{i,j}^{(s)}(t_w, t_w) = +\frac{1}{4} (\delta_{j,i_1} + \delta_{j,i_1-1}) \langle e | \hat{n}_{i_1-1} \hat{n}_{i_1} E_{i_1+1,i_2} e^{W^c t_w} | 1 \rangle \\ + \frac{1}{4} (\delta_{j,i_2} + \delta_{j,i_2-1}) \langle e | E_{i_1,i_2-1} \hat{n}_{i_2-1} \hat{n}_{i_2} e^{W^c t_w} | 1 \rangle. \quad (81)$$

Due to the difference in signs between Eqs. (71) and (79) we end up with a single domain density $D_{i_2-i_1}(t_w)$ in the symmetric response Eq. (80) rather than the sum we had in the asymmetric case Eq. (73). This has important consequences for the scaling behaviour of $R_{i,j}^{(s)}(t_w, t_w)$. The excess term $\Delta_{i,j}^{(s)}(t_w, t_w)$, Eq. (81), differs from $\Delta_{i,j}^{(a)}(t_w, t_w)$, Eq. (74), only in overall signs; we therefore discuss both quantities together in Appendix B. At fixed $i_2 - i_1$ and large t_w we have, for instance, that both $\Delta_{i,j}^{(a)}(t_w, t_w)$ and $\Delta_{i,j}^{(s)}(t_w, t_w)$ scale like $\mathcal{O}(1/t_w^{3/2})$. This is a subdominant contribution to $R_{i,j}^{(a)}(t_w, t_w) = \mathcal{O}(1/t_w^{1/2})$, while in $R_{i,j}^{(s)}(t_w, t_w) = \mathcal{O}(1/t_w^{3/2})$ from Eq. (80) it contributes to leading order. Therefore the scaling of $R_{i,j}^{(s)}(t_w, t_w)$ for small $i_2 - i_1 \geq 1$ and large t_w depends on the precise coagulation rate and so is different in the effective FA model and e.g. free fermion DLPC. Only in the regime $i_2 - i_1 \gg 1$ does $R_{i,j}^{(s)}(t_w, t_w)$ assume a robust scaling form that is independent of the underlying coagulation rate. This is because the density of domains $D_n(t_w)$ has

a robust scaling in this regime while at the same time $\Delta_{i,j}^{(s)}(t_w, t_w)$ becomes negligible in comparison (see Appendix B). Having clarified the range of validity of Eq. (80) we now substitute the free fermion DLPC result Eq. (43) for the domain density,

$$R_{i,j}^{(s)}(t_w, t_w) = -\frac{1}{4}B_{i,j}e^{-2t_w}[I_{i_2-i_1-1} - I_{i_2-i_1+1}](2t_w) + \Delta_{i,j}^{(s)}(t_w, t_w). \quad (82)$$

Inserting this expression into Eq. (63) produces the associated two-time response function. As for the asymmetric case the k -summations may be carried out using the convolution property Eq. (A.5) of the modified Bessel functions. The symmetric part of the two-time response function Eq. (61) with $n = i - j$ becomes

$$R_n^{(s)}(t, t_w) = -\frac{1}{4}e^{-2t} \{I_n(t - t_w)[-I_{n-2} + 2I_n - I_{n+2}](t + t_w) + [I_{n-1} - I_{n+1}](t - t_w)[I_{n-1} - I_{n+1}](t + t_w)\} + \Delta_n^{(s)}(t, t_w). \quad (83)$$

This result is exact for free fermion DLPC; its leading order scaling at large t_w applies more generally for arbitrary coagulation rates as long as $\Delta t \gg 1$. The latter holds true since for $\Delta t \gg 1$ the Green's function in Eq. (63) picks up its leading contributions from $k_2 - k_1 = \mathcal{O}(\sqrt{\Delta t})$, and in this regime Eq. (82) has a robust long-time scaling form.

4. Local Correlation and Response

In this section we study the nonequilibrium FDT in the FA model associated with the local defect observable $A = \hat{n}_i$. Before presenting results for the FDR we discuss the dynamics of the corresponding connected two-time local defect autocorrelation and response functions, denoted by $C_d(t, t_w)$ and $R_d(t, t_w)$, respectively.

4.1. Defect Autocorrelation

The defect autocorrelation function $C_d(t, t_w) = \langle \hat{n}_i(t)\hat{n}_i(t_w) \rangle - \langle \hat{n}_i(t) \rangle \langle \hat{n}_i(t_w) \rangle = C_0(t, t_w)$ is given by Eq. (60) evaluated for $n = 0$,

$$C_d(t, t_w) = e^{-2t_w}[I_0 + I_1](2t_w) \sum_{p,q=0}^{\infty} G_{(0,1),(-p,q+1)}^{(2)}(\Delta t) H_{p+q+1}(2t_w) - 2 \sum_{p,q=0}^{\infty} G_{(0,-1),(p,q)}^{(2)}(\Delta t) e^{-2t_w}[I_p + I_{p+1}](2t_w) [\delta_{q,0} + H_q(2t_w)]. \quad (84)$$

Equation (84) is an exact expression for the connected two-time particle autocorrelation in the free fermion DLPC process with filled initial state. Asymptotically, for $t_w \rightarrow \infty$, it applies for DLPC processes with arbitrary coagulation rate and homogeneous initial states with finite particle density. We add that Eq. (84) is then exact to leading order in t_w for arbitrary $\Delta t \geq 0$, i.e. including small $\Delta t = O(1)$. This is because at large t_w , the correlation function for Δt of $O(1)$ is to leading order unaffected by coagulation processes, the typical distances of $O(\sqrt{t_w})$ between particles being too large for them to meet. For $\Delta t = O(t_w)$, on the other hand, coagulation events do play a role but the precise extent of their $O(1)$ durations is irrelevant. Either way, the dynamics of the

DLPC process is essentially controlled by diffusion and independent of the coagulation rate [56].

Let us now discuss some limiting cases of Eq. (84). For $\Delta t = 0$, one has $G_{i,j}^{(2)}(0) = \delta_{i_1-j_1}\delta_{i_2-j_2} - \delta_{i_1-j_2}\delta_{i_2-j_1}$ and so only the $p = q = 0$ term from the first sum remains while the second one vanishes altogether. Using $H_1(2t_w) = 1 - e^{-2t_w}[I_0 + I_1](2t_w)$, see Eq. (A.9), we obtain

$$C_d(t_w, t_w) = c(t_w) - c^2(t_w), \quad (85)$$

with $c(t_w) = \langle \hat{n}_i(t_w) \rangle$ the defect concentration given in Eq. (44). This result is consistent with the definition of $C_d(t, t_w)$ as it must be. In the quasi-equilibrium regime $\Delta t \geq 0$ fixed and $t_w \rightarrow \infty$, convergence of the sums in Eq. (84) is guaranteed by the Green's functions, with relevant contributions originating from $p, q = \mathcal{O}(1)$. We may therefore substitute the asymptotic expansions Eqs. (A.6) and (A.10) for the t_w -dependent functions,

$$C_d(t, t_w) \sim \frac{1}{\sqrt{\pi t_w}} \sum_{p,q=0}^{\infty} \left[G_{(0,1),(-p,q+1)}^{(2)}(\Delta t) - 2G_{(0,-1),(p,q)}^{(2)}(\Delta t) \right]. \quad (86)$$

After substitution of Eq. (48) for the Green's functions the double sum factorizes. There are several cancellations and only one sum of the type Eq. (A.1) remains. We find

$$C_d(t, t_w) \sim \frac{1}{\sqrt{\pi t_w}} e^{-\Delta t} I_0(\Delta t) \sim c(t_w) p_r(\Delta t). \quad (87)$$

Here we have identified the probability of return to the origin for a standard random walker, $p_r(\tau) = e^{-\tau} I_0(\tau)$. The leading contribution to the two-time correlation arises from $C_d(t, t_w) \sim \langle \hat{n}_i(t) \hat{n}_i(t_w) \rangle$ and its value is thus given by the probability $c(t_w)$ of having a defect at site i at time t_w multiplied by the probability $p_r(t - t_w)$ for this defect to return and occupy the same site at time t . This reasoning confirms the intuition that in the quasi-equilibrium regime defects are too far from each other to meet and react and so behave as isolated random walkers; this argument of course applies to both DLPC and DLPA [20, 37].

Finally we consider the aging regime $\Delta t, t_w \gg 1$ with the time ratio $\Delta t/t_w$ fixed and finite. Here asymptotic expansions of the Green's functions in Eq. (84) are required,

$$G_{(0,1),(-p,q+1)}^{(2)}(\Delta t) = e^{-2\Delta t} [I_p I_q - I_{p+1} I_{q+1}](\Delta t), \quad (88)$$

$$G_{(0,-1),(p,q)}^{(2)}(\Delta t) = e^{-2\Delta t} [I_p I_{q+1} - I_{p+1} I_q](\Delta t). \quad (89)$$

Some care has to be taken since the leading contributions of the modified Bessel functions cancel. To obtain the first subdominant correction we rewrite

$$I_{p+1}(\Delta t) = \frac{1}{2}[I_{p-1} + I_{p+1}](\Delta t) - \frac{1}{2}[I_{p-1} - I_{p+1}](\Delta t) = \partial_{\Delta t} I_p(\Delta t) - \frac{p}{\Delta t} I_p(\Delta t), \quad (90)$$

where in the second equality Eqs. (A.3) and (A.4) were used. The asymptotically dominant terms in the sums in Eq. (84) satisfy $p^2/\Delta t = \mathcal{O}(1)$. We then note that from the scaling Eq. (A.7) one has $\partial_{\Delta t} I_p(\Delta t) = I_p(\Delta t) [1 + \mathcal{O}(1/\Delta t)]$ and, via Eq. (90),

$I_{p+1}(\Delta t) = I_p(\Delta t) [1 - p/\Delta t + \mathcal{O}(1/\Delta t)]$. From this the leading terms in the Green's functions are

$$G_{(0,1),(-p,q+1)}^{(2)}(\Delta t) \sim \frac{p+q}{\Delta t} e^{-2\Delta t} I_p(\Delta t) I_q(\Delta t), \quad (91)$$

$$G_{(0,-1),(p,q)}^{(2)}(\Delta t) \sim \frac{p-q}{\Delta t} e^{-2\Delta t} I_p(\Delta t) I_q(\Delta t). \quad (92)$$

The aging expansion of $C_d(t, t_w)$ follows by substituting this into Eq. (84) and using the scalings Eqs. (A.6), (A.7) and (A.11) for the functions I_n and H_n . The summations in Eq. (84) then take the form $(1/t_w) \sum_{p,q \geq 0} f(p/\sqrt{t_w}, q/\sqrt{t_w})$ and become integrals in the aging limit,

$$C_d(t, t_w) \sim \frac{4}{\pi^{3/2}} \frac{t_w}{\Delta t^2} \int_0^\infty dx \int_0^\infty dy (x+y) e^{-(2t_w/\Delta t)(x^2+y^2)} \Phi(x+y) \\ - \frac{8}{\pi^{3/2}} \frac{t_w}{\Delta t^2} \int_0^\infty dx \int_0^\infty dy (x-y) e^{-(2t_w/\Delta t)(x^2+y^2)} e^{-x^2} \Phi(y) \quad (93)$$

with $\Phi(\cdot)$ the complementary error function as defined in Eq. (A.11). The integrals in this expression have elementary solutions [57]. One shows that

$$C_d(t, t_w) \sim \frac{1}{\pi} \frac{1}{t+t_w} \left[\sqrt{\frac{t+t_w}{t-t_w}} - 1 \right. \\ \left. + \frac{2}{\pi} \sqrt{\frac{t-t_w}{2t_w}} \arccos \sqrt{\frac{t-t_w}{t+t_w}} - \frac{1}{\pi} \frac{t+t_w}{\sqrt{t t_w}} \arccos \frac{t-t_w}{t+t_w} \right]. \quad (94)$$

This is the exact scaling of $C_d(t, t_w)$ in the aging limit $\Delta t, t_w \rightarrow \infty$ at fixed and finite $\Delta t/t_w$. As emphasised above, it applies not only for free fermion DLPC but any diffusion coagulation process with finite coagulation rate, including in particular the FA model. The result Eq. (94) takes a simple form in the limiting cases

$$\Delta t \ll t_w : C_d(t, t_w) \approx \frac{1}{\pi \sqrt{2 \Delta t t_w}}, \quad (95)$$

$$\Delta t \gg t_w : C_d(t, t_w) \approx \frac{3\pi - 8}{3\pi^2} \frac{t_w}{\Delta t^2}. \quad (96)$$

As expected, the $\Delta t \ll t_w$ limit Eq. (95) matches the expansion for $\Delta t \gg 1$ of the quasi-equilibrium result Eq. (87). Plots of the scaling function (94) are shown in Fig. 1 below and illustrate the crossover from the scaling (95) to (96).

It is interesting to compare the above scaling of $C_d(t, t_w)$ in DLPC to the corresponding result $C_{d,A}(t, t_w)$ for DLPA. The latter was derived in [20] and reads §

$$C_{d,A}(t, t_w) \sim \frac{1}{2\pi} \frac{1}{\sqrt{t+t_w}} \left[\frac{1}{\sqrt{t-t_w}} - \frac{1}{\sqrt{t+t_w}} \right]. \quad (97)$$

Plots of this are also displayed in Fig. 1 below and demonstrate that the defect autocorrelation functions in DLPC and DLPA are qualitatively very similar. Quantitatively, the limit forms of Eq. (97) are

$$\Delta t \ll t_w : C_{d,A}(t, t_w) \approx \frac{1}{2\pi \sqrt{2 \Delta t t_w}}, \quad (98)$$

§ Note that $C_d(t, t_w)$ in [20] is defined in terms of the observable $A = \sigma_i^z \sigma_{i+1}^z$ and thus differs from the present choice $A = \hat{n}_i = \frac{1}{2}(1 - \sigma_i^z \sigma_{i+1}^z)$ by a factor 4; the same applies for response functions.

$$\Delta t \gg t_w : C_{d,A}(t, t_w) \approx \frac{1}{2\pi} \frac{t_w}{\Delta t^2}. \quad (99)$$

From Eqs. (95,98) we observe that $C_{d,A}(t, t_w) \approx \frac{1}{2}C_d(t, t_w)$ in the regime $\Delta t \ll t_w$. This is a direct consequence of the quasi-equilibrium behaviour Eq. (87), which applies for DLPC as well as DLPA, and the fact that defect concentrations are related by $\langle \hat{n}_i(t_w) \rangle_a = \frac{1}{2} \langle \hat{n}_i(t_w) \rangle_c$, c.f. Eq. (31). But in the opposite regime $\Delta t \gg t_w$ one finds $C_{d,A}(t, t_w) \approx r C_d(t, t_w)$ with $r = 3\pi/(6\pi - 16) \approx 3.31$ from Eqs. (96,99). Here defects interact and we thus expect that the nontrivial ratio r is determined by genuine many body effects. These must clearly differ between DLPC and DLPA, given that – amongst other things – the two processes have different scaling forms for their domain size distributions [55].

4.2. Local Response Function

According to Eq. (68) the two-time defect autoresponse function in the FA model may be decomposed into two contributions $R_d(t, t_w) = R_d^{(a)}(t, t_w) + R_d^{(s)}(t, t_w)$. As the asymmetric and symmetric perturbations have very different effects on the local defect dynamics we discuss the corresponding response functions separately.

4.2.1. Asymmetric Perturbation The two-time defect autoresponse to the asymmetric part of the perturbation is given by Eq. (76) with $n = 0$,

$$R_d^{(a)}(t, t_w) = \partial_{t_w} e^{-2t} I_0(t - t_w) [I_0 + I_1](t + t_w) + \Delta_0^{(a)}(t, t_w). \quad (100)$$

The correction $\Delta_0^{(a)}(t, t_w)$ is subdominant at large t_w and for any $\Delta t \geq 0$ and will therefore be neglected in the following. Due to the explicit t_w -derivative in Eq. (100) the corresponding step response function can be obtained directly as

$$\chi_d^{(a)}(t, t_w) = \int_{t_w}^t d\tau R_d^{(a)}(t, \tau) \sim e^{-2t} \{ [I_0 + I_1](2t) - I_0(t - t_w) [I_0 + I_1](t + t_w) \}. \quad (101)$$

Plots of $\chi_d^{(a)}(t, t_w)$ are shown in Fig. 1 below. This result is interesting in various ways. Consider first the quasi-equilibrium behaviour at fixed $\Delta t \geq 0$ and large t_w ,

$$\chi_d^{(a)}(t, t_w) \sim \frac{1}{\sqrt{\pi t_w}} [1 - e^{-\Delta t} I_0(\Delta t)] \sim c(t_w) [1 - p_r(\Delta t)], \quad (102)$$

to leading order in t_w . The form of Eq. (102) reflects a simple mechanism: at time t_w there is a homogeneous concentration $c(t_w)$ of defects in the system. But application of the asymmetric perturbation $V_i^{(a)}$, which traps diffusing defects on site i , yields an increase of $\langle \hat{n}_i(t) \rangle$ as given by Eq. (102). The step response $\chi_d^{(a)}(t, t_w)$ approaches $c(t_w)$ within a time interval $\Delta t = \mathcal{O}(1)$, see Fig. 1. In the aging regime, where both Δt and t_w are large and comparable, one has from Eq. (101) that $\chi_d^{(a)}(t, t_w) \sim c(t)$. The step response then decreases along with the density of defects in the system. This explains the non-monotonic shape of $\chi_d^{(a)}(t, t_w)$ shown in Fig. 1.

It is important to note that $\chi_d^{(a)}(t, t_w)$ is dominated by the small- Δt behaviour of $R_d^{(a)}(t, t_w)$. Indeed, in the quasi-equilibrium regime Eq. (102) reproduces

$$R_d^{(a)}(t, t_w) = -\partial_{t_w} \chi_d^{(a)}(t, t_w) \sim -c(t_w) \partial_{\Delta t} p_r(\Delta t), \quad (103)$$

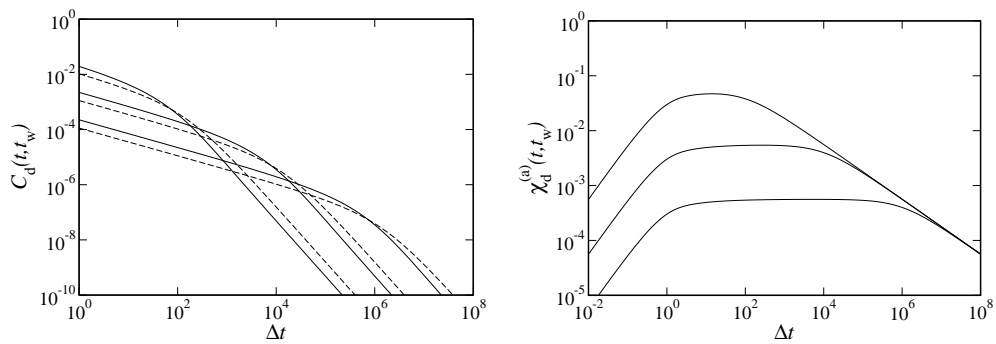


Figure 1. Left panel: scaling form of the two-time defect autocorrelation $C_d(t, t_w)$, Eq. (94), in the FA model for $t_w = 10^2, 10^4$ and 10^6 (full lines) and, for comparison, the corresponding DPLA result Eq. (97) at the same values of t_w (dashed lines). Right panel: plots of the step response $\chi_d^{(a)}(t, t_w)$ to the asymmetric part of the perturbation, Eq. (101), for $t_w = 10^2, 10^4$ and 10^6 from top to bottom, respectively.

consistent with Eq. (100); this result is positive since $p_r(\Delta t)$ is a decreasing function of Δt and hence $-\partial_{\Delta t} p_r(\Delta t) > 0$. But in the aging regime $\chi_d^{(a)}(t, t_w) \sim c(t)$ to leading order as discussed above, which would naively suggest $R_d^{(a)}(t, t_w) = -\partial_{t_w} c(t) = 0$. More precisely it means that the aging part of $R_d^{(a)}(t, t_w)$ only contributes subdominantly to $\chi_d^{(a)}(t, t_w)$. From the full expression Eq. (101), or equivalently Eq. (100), one deduces that in fact

$$R_d^{(a)}(t, t_w) \sim \frac{1}{2\pi} \left[\frac{1}{\sqrt{t + t_w}(t - t_w)^{3/2}} - \frac{1}{\sqrt{t - t_w}(t + t_w)^{3/2}} \right]. \quad (104)$$

For $\Delta t \ll t_w$ the first term in Eq. (104) dominates, matching the large Δt behaviour of the quasi-equilibrium result Eq. (103). For $\Delta t \gg t_w$, on the other hand, the terms in Eq. (104) cancel to leading order in $t_w/\Delta t$; then $R_d^{(a)}(t, t_w) \approx t_w/(\pi \Delta t^3)$.

We add that a response function analogous to $R_d^{(a)}(t, t_w)$ was calculated for DLPA in [20]. Denoting the latter by $R_{d,A}(t, t_w)$ one has from [20] that $R_{d,A}(t, t_w) = \frac{1}{2} R_d^{(a)}(t, t_w)$. In terms of the two-time defect autoresponse for an asymmetric perturbation there is therefore no distinction between DLPC and DLPA, except for the factor of $\frac{1}{2}$ which has its origin in $\langle \hat{n}_i(t_w) \rangle_a = \frac{1}{2} \langle \hat{n}_i(t_w) \rangle_c$, see Eq. (31).

4.2.2. Symmetric Perturbation Setting $n = 0$ in Eq. (83) gives for the autoresponse to the symmetric part of the perturbation,

$$R_d^{(s)}(t, t_w) = -\frac{1}{2} e^{-2t} I_0(t - t_w) [I_0 - I_2](t + t_w) + \Delta_0^{(s)}(t, t_w). \quad (105)$$

As discussed in Sec. 3.2.2 the behaviour for short time differences $\Delta t = \mathcal{O}(1)$ of this result does depend on the precise coagulation rate. So in this regime Eq. (105) applies to free fermion DLPC but not the FA model. This does not constitute a problem, however, since Eq. (105) scales as $\mathcal{O}(t_w^{-3/2})$ at large t_w and fixed Δt . It is therefore subdominant against the short-time scaling of the asymmetric response Eq. (103). Only in the aging regime does the symmetric response contribute significantly to the overall

response function; there it is independent of the coagulation rate as explained above and so does apply to the FA model. Taking the appropriate limits in Eq. (105) gives

$$R_d^{(s)}(t, t_w) \sim -\frac{1}{2\pi} \frac{1}{\sqrt{t-t_w} (t+t_w)^{3/2}}. \quad (106)$$

For $\Delta t \ll t_w$ this simplifies to $R_d^{(s)}(t, t_w) \approx -1/[2\pi\sqrt{\Delta t}(2t_w)^{3/2}]$ while for $\Delta t \gg t_w$ one has $R_d^{(s)}(t, t_w) \approx -1/(2\pi\Delta t^2)$. Note the overall *negative* sign of the response: to understand this result qualitatively recall that the symmetric perturbation $V_i^{(s)}$ increases the local diffusion rates between sites $i-1 \rightleftharpoons i \rightleftharpoons i+1$. A response can only occur if a defect is present on one of these sites at time t_w . During the time interval where the perturbation is applied the dynamics of this defect are accelerated. In and by itself this does not have any effect on the defect concentration $\langle \hat{n}_i(t) \rangle$ at site i . However, the “extra time” for the defect manifests itself through the fact that it will now coagulate earlier with a neighbouring defect. The local concentration is therefore reduced, and this explains the negative sign of the response. Physically this behaviour derives from the activated character of the FA dynamics [38]. The increased local diffusion rates in the effective FA model represent locally reduced energy barriers for the creation of defects. In equilibrium this would increase the defect density; out of equilibrium the dominant effect is a speeding up of the relaxation of the defect density towards zero, leading to a reduction in the number of defects.

The scaling of the step response function $\chi_d^{(s)}(t, t_w)$ in the aging regime is obtained correctly by integration of Eq. (106), the reason being that small- Δt contributions from $R_d^{(s)}(t, t_w)$ only amount to subdominant corrections in the integral. Thus,

$$\chi_d^{(s)}(t, t_w) = \int_{t_w}^t d\tau R_d^{(s)}(t, \tau) \sim -\frac{1}{2\pi} \frac{\sqrt{t-t_w}}{t\sqrt{t+t_w}}, \quad (107)$$

in the aging regime $\Delta t, t_w \gg 1$ with fixed and finite $\Delta t/t_w$. For $\Delta t \ll t_w$ this reduces to $\chi_d^{(s)}(t, t_w) \approx -\sqrt{\Delta t}/(2\sqrt{2}\pi t_w^{3/2})$ while for $\Delta t \gg t_w$ one finds $\chi_d^{(s)}(t, t_w) \approx -1/(2\pi\Delta t)$. Comparison of Eq. (107) with Eq. (101) shows that the overall step response in the aging regime $\chi_d(t, t_w) = \chi_d^{(a)}(t, t_w) + \chi_d^{(s)}(t, t_w) \sim c(t)$ is dominated by the short- Δt behaviour of $R_d^{(a)}(t, t_w)$ as discussed above. The aging parts of $R_d^{(a)}(t, t_w)$, Eq. (104), and $R_d^{(s)}(t, t_w)$, Eq. (106), are both of the same order but only contribute subdominantly in the overall step response $\chi_d(t, t_w)$. The consequences of this will become clear below.

4.3. FDR and FD plot

Based on the above results for connected two-time defect autocorrelation and response functions one immediately obtains the associated fluctuation-dissipation (FD) plots. We use normalized FD plots [20, 59, 60] of $\tilde{\chi}(t, t_w) = \chi(t, t_w)/C(t, t)$ versus $1 - \tilde{C}(t, t_w)$ where $\tilde{C}(t, t_w) = C(t, t_w)/C(t, t)$. Normalization scales the plot so that the abscissa always lies in the range from zero to one. It is crucial that the plot is parameterised by t_w with t held fixed [19, 59]. Only then is the slope of the plot guaranteed to be $X(t, t_w)$ as one readily verifies from Eq. (3) and $R(t, t_w) = -\partial_{t_w}\chi(t, t_w)$.

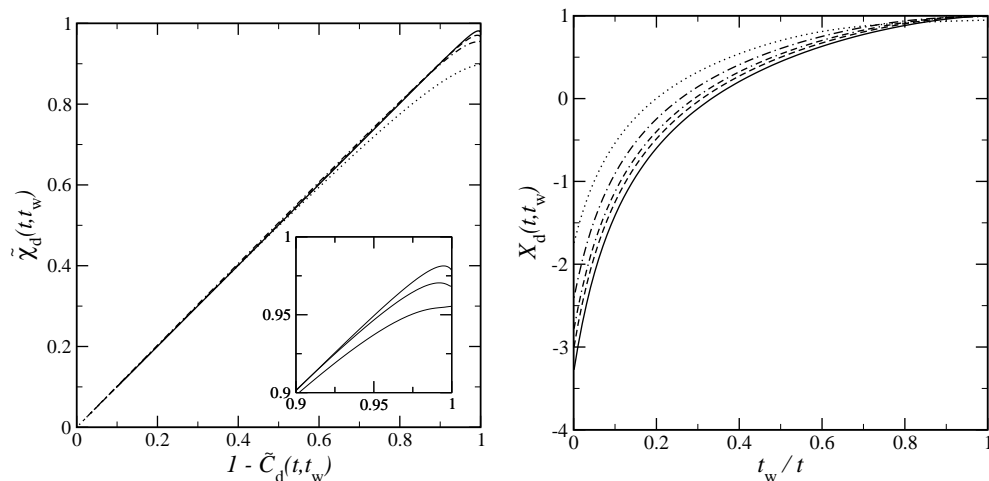


Figure 2. Left: Normalised FD plot for the local defect observable $A = \hat{n}_i$. Data were obtained by numerical evaluation [58] of the full expressions (84), (100), (105) at $t = 10^{1/2}, 10^1, 10^{3/2}, 10^2$ with $t_w \in [0, t]$. For increasing t the curves move upwards, converging to the equilibrium line of unit slope. Inset: The data in the top-right corner on a magnified scale, not containing the $t = 10^{1/2}$ curve. Right: Plot of the FDR $X_d(t, t_w)$ versus t_w/t for $t_w = 10^{1/2}$ (dotted), $10^1, 10^{3/2}, 10^2$ and ∞ (full line). The curves for finite t_w were again obtained by numerical evaluation of the full expressions while the limit curve follows from the scaling forms (94), (104) and (106).

The FD plot for the local defect observable in the FA model is shown in Fig. 2. It quickly converges to the equilibrium line $\tilde{\chi}_d = 1 - \tilde{C}_d$, consistently with observations made in computer simulations [21, 36]. However, a plot of the FDR $X_d(t, t_w)$, also shown in Fig. 2, clearly demonstrates that equilibrium FDT is *not* satisfied. In fact $X_d(t, t_w)$ steadily decreases with increasing t and actually turns *negative* around $t_w/t \approx 1/3$. This is reflected in the FD plot, which bends down as $\tilde{C}_d \rightarrow 0$. The plot of $X_d(t, t_w)$ also indicates that a nontrivial scaling form $X_d(t, t_w) \sim X_d(t_w/t)$ exists in the aging limit; we return to this below.

In order to understand the shape of the FD plot let us first consider the dynamics in the quasi-equilibrium regime of large t_w but finite $\Delta t \geq 0$. Here $C_d(t, t_w) \sim c(t_w)p_r(\Delta t)$ as given by Eq. (87) and $\chi_d(t, t_w) \sim \chi_d^{(a)}(t, t_w) \sim c(t_w)[1 - p_r(\Delta t)]$, Eq. (102), is dominated by the asymmetric perturbation. To leading order in t_w we then have for the normalized quantities $\tilde{\chi}_d = 1 - \tilde{C}_d = 1 - p_r(\Delta t)$ and equilibrium FDT is satisfied. Furthermore, since $\tilde{C}_d \sim p_r(\Delta t)$ becomes negligibly small already in the $\Delta t = \mathcal{O}(1)$ time sector, aging effects are compressed into the top right corner of the FD plot. Asymptotically only the quasi-equilibrium regime is visible in the FD plot [20, 37, 38].

Consider next the aging regime where both Δt and t_w are large, but with a finite ratio $\Delta t/t_w$. The normalized correlation then is $\tilde{C}_d = \mathcal{O}(1/\sqrt{t})$. The dominant scaling of the step response $\chi_d \sim c(t)$ would give $\tilde{\chi}_d = 1$. This is modified by aging contributions from $R_d^{(a)}(t, t_w)$ and $R_d^{(s)}(t, t_w)$ so that $1 - \tilde{\chi}_d = \mathcal{O}(1/\sqrt{t})$. In the FD plot, aging effects are only visible in a region of size $\mathcal{O}(1/\sqrt{t})$ in the top right corner of the plot; this regime is highlighted in the inset of Fig. 2. Effects of the asymmetric perturbation

alone, which are accounted for in $\chi_d^{(a)}(t, t_w)$, Eq. (101), would cause the plot to turn horizontal with $X^\infty = 0$; this would be the analog of the DLPA result in [20]. However, the additional *negative* contribution of $\chi_d^{(s)}(t, t_w)$, Eq. (107), in the overall step response $\chi_d(t, t_w) = \chi_d^{(a)}(t, t_w) + \chi_d^{(s)}(t, t_w)$ makes the plot non-monotonic with $X^\infty < 0$, which is consistent with simulations [38]. Note that this non-monotonicity is genuine and *not* due to incorrect parameterisation of the plot with t instead of t_w [13].

The above discussion shows that for defect observables an FD plot gives a rather unsatisfactory graphical representation of the FDT violation in the FA model. It is more appropriate to look instead directly at the time dependence of the FDR $X_d(t, t_w)$, as shown in Fig. 2. The FDR involves the response functions $R_d^{(a)}(t, t_w)$ and $R_d^{(s)}(t, t_w)$. In contrast to the associated step response functions, these are not dominated only by the quasi-equilibrium dynamics at small Δt and so can reveal genuine aging effects. Looking at the relative importance of the asymmetric and symmetric contributions, one sees that in the aging regime $\Delta t, t_w \gg 1$ with $\Delta t/t_w = \mathcal{O}(1)$ both $R_d^{(a)}(t, t_w)$, Eq. (104), and $R_d^{(s)}(t, t_w)$, Eq. (106), are of the same order $\mathcal{O}(1/t_w^2)$. Keeping in mind that $R_d^{(a)}(t, t_w) > 0$ while $R_d^{(s)}(t, t_w) < 0$ and looking at the plot of $X_d(t, t_w)$ in Figure 2, we notice that $R_d^{(s)}(t, t_w)$ in fact becomes dominant for $\Delta t \gg t_w$; explicitly, $R_d^{(s)}(t, t_w) \approx -1/(2\pi\Delta t^2)$ while $R_d^{(a)}(t, t_w) \approx t_w/(\pi\Delta t^3) = \mathcal{O}((t_w/\Delta t)|R_d^{(s)}(t, t_w)|)$. This causes the change of sign in $R_d(t, t_w)$ and thus $X_d(t, t_w)$. So, while in the $\Delta t \ll t_w$ limit the response is dominated by the trapping effect of the asymmetric part of the perturbation, it is the speedup effect of the local dynamics through the symmetric component of the perturbation that dominates for $\Delta t \gg t_w$. This speedup is the consequence of coupling of the observable to energy barriers in the activated dynamics of the FA model.

By working out the scaling of $\partial_{t_w} C_d(t, t_w)$ from Eq. (94) and using the results Eqs. (104, 106) one obtains the scaling form of $X_d(t, t_w)$. We do not state the explicit result since it is somewhat bulky; importantly, however, its time dependence is only via the ratio t_w/t . A plot of $X_d(t_w/t)$ is contained in Figure 2. It crosses over from $X_d = 1$ in the quasi-equilibrium limit to $X_d = X_d^\infty$ for $t \gg t_w$; the asymptotic FDR is

$$X_d^\infty = -\frac{3\pi}{6\pi - 16} \approx -3.307. \quad (108)$$

We recall that the results shown in Fig. 2 are fully exact for the free fermion DLPC process (with filled initial state). In the limit of large t_w , where the precise coagulation rate and initial state density become irrelevant, the results – including the scaling form of $X_d(t_w/t)$ and the value X_d^∞ – apply to arbitrary DLPC processes and, in particular, to the FA model. Finite time data were included in Figure 2 only in order to give an indication of the speed of convergence (for free fermion DLPC) to the long-time asymptotic results.

5. Global Correlation and Response

Given that the FA model can be viewed as a coarsening system, and following the philosophy of [20], we now analyse the nonequilibrium FDT for the global observable $A = \sum_i \hat{n}_i$, which is nothing but the energy. Our expectations are, firstly, that we should find the same X^∞ as for the local defect observable [20, 35] and, secondly, that a nontrivial limit FD plot should exist in this case [20, 60, 61]. As above we first study separately the connected two-time energy correlation and response functions $C_e(t, t_w)$ and $R_e(t, t_w)$, respectively; both will be normalised by $1/N$ to get quantities of order unity. Then the resulting FDR and FD plot are discussed.

5.1. Energy Correlation

We obtain an expression for $C_e(t, t_w)$ by summing Eq. (60) over n since, using translational invariance, $C_e(t, t_w) = (1/N) \sum_{i,j} [\langle \hat{n}_i(t) \hat{n}_j(t_w) \rangle - \langle \hat{n}_i(t) \rangle \langle \hat{n}_j(t_w) \rangle] = \sum_n C_n(t, t_w)$. Via the convolution property Eq. (A.5) one readily shows that

$$\sum_n G_{(n, n+1), (-p, q+q)}^{(2)}(\Delta t) = e^{-2\Delta t} [I_{p+q} - I_{p+q+2}](2\Delta t), \quad (109)$$

$$\sum_n G_{(\pm n, \pm n-1), (p, q)}^{(2)}(\Delta t) = e^{-2\Delta t} [I_{p-q-1} - I_{p-q+1}](2\Delta t). \quad (110)$$

Thus we have from Eq. (60)

$$C_e(t, t_w) = e^{-2t} [I_0 + I_1](2t_w) \sum_{p, q=0}^{\infty} [I_{p+q} - I_{p+q+2}](2\Delta t) H_{p+q+1}(2t_w) - 2 \sum_{p, q=0}^{\infty} e^{-2t} [I_{p-q-1} - I_{p-q+1}](2\Delta t) [I_p + I_{p+1}](2t_w) [\delta_{q,0} + H_q(2t_w)]. \quad (111)$$

The energy correlation function $C_e(t, t_w)$ is constant – with respect to Δt – in the quasi-equilibrium regime. This is obvious when considering that defects are typically a distance $\mathcal{O}(\sqrt{t_w})$ apart and can therefore not meet within a time interval $\Delta t = \mathcal{O}(1)$. Thus no coagulation processes are possible and the energy remains constant. It is somewhat awkward to derive this directly from Eq. (111) because the double sum in the second line only reduces to a one-dimensional sum; the assumption $\Delta t = \mathcal{O}(1)$ imposes merely that $p - q$ must be of $\mathcal{O}(1)$ to get a significant contribution. One can get the result indirectly, however, by first going to the aging regime and then considering the limit $\Delta t \ll t_w$ (see below). The correlation function at $\Delta t = 0$ itself, which gives the energy fluctuations, is much simpler to work out using $I_n(0) = \delta_{n,0}$. In this case it can be shown that

$$C_e(t_w, t_w) = 3e^{-2t_w} [I_0 + I_1](2t_w) - e^{-4t_w} [3I_0 + 4I_1 + I_2](4t_w) \quad (112)$$

An aging expansion of Eq. (111) is obtained rather easily using Eqs. (A.4), (A.6), (A.7) and (A.11). In the aging limit the double sums turn into integrals and one finds

$$C_e(t, t_w) \sim \frac{4}{\pi} \frac{t_w}{\Delta t^{3/2}} \int_0^\infty dx \int_0^\infty dy (x+y) e^{-(t_w/\Delta t)(x+y)^2} \Phi(x+y)$$

$$-\frac{8}{\pi} \frac{t_w}{\Delta t^{3/2}} \int_0^\infty dx \int_0^\infty dy (x-y) e^{-(t_w/\Delta t)(x-y)^2} e^{-x^2} \Phi(y). \quad (113)$$

Again there are elementary solutions to these integrals [57], giving

$$C_e(t, t_w) \sim \frac{2}{\sqrt{\pi}} \left[\frac{1}{\sqrt{t}} - \frac{1}{\sqrt{t+t_w}} - \frac{\sqrt{t-t_w}}{\pi t} \right] + \frac{2}{\pi^{3/2}} \left[\frac{1}{\sqrt{t_w}} \arcsin \sqrt{\frac{t_w}{t}} - \frac{2}{\sqrt{t+t_w}} \arcsin \frac{t_w}{t} \right]. \quad (114)$$

This leading order long-time scaling applies to all DLPC processes with finite coagulation rate in the limit $t_w \gg 1$ and for any $\Delta t \geq 0$. Coagulation rate effects are in principle present for $\Delta t = \mathcal{O}(1)$ but are subleading for large t_w because they are driven by the density of small domains. For $\Delta t \ll t_w$ the expression (114) approaches a constant value as anticipated and matches up with the large- t_w expansion of the equal-time value, Eq. (112). Specifically, the limit forms of Eq. (114) are,

$$\Delta t \ll t_w : C_e(t, t_w) \approx \frac{3 - 2\sqrt{2}}{\sqrt{\pi t_w}}, \quad (115)$$

$$\Delta t \gg t_w : C_e(t, t_w) \approx \frac{3\pi - 8}{3\pi^{3/2}} \frac{t_w}{\Delta t^{3/2}}. \quad (116)$$

Figure 3 below shows plots of the scaling function Eq. (114), illustrating the crossover from the plateau Eq. (115) to the long time scaling Eq. (116).

In analogy with the discussion in Sec. 4.1 we again compare the scaling Eq. (114) of $C_e(t, t_w)$ in DLPC with the corresponding result $C_{e,A}(t, t_w)$ in DLPA. From Ref. [20],

$$C_{e,A}(t, t_w) \sim \frac{1}{\sqrt{\pi}} \left(\frac{1}{\sqrt{t}} - \frac{1}{\sqrt{t+t_w}} \right), \quad (117)$$

bearing in mind that the result in [20] contains an extra factor 4. Plots of Eq. (117) are also included in Fig. 3 below, and cross over between the limits

$$\Delta t \ll t_w : C_{e,A}(t, t_w) \approx \frac{2 - \sqrt{2}}{2\sqrt{\pi t_w}}, \quad (118)$$

$$\Delta t \gg t_w : C_{e,A}(t, t_w) \approx \frac{1}{2\sqrt{\pi}} \frac{t_w}{\Delta t^{3/2}}. \quad (119)$$

In the regime $\Delta t \ll t_w$ we can again establish a simple relationship between the functions $C_{e,A}(t, t_w)$ and $C_e(t, t_w)$. It is sufficient to consider the instantaneous energy fluctuations for $t = t_w$ since both functions are, to leading order, independent of Δt when $\Delta t \ll t_w$. Now, by definition $C_{e,A}(t_w, t_w) = (1/N) \sum_{i,j} [\langle \hat{n}_i(t_w) \hat{n}_j(t_w) \rangle_a - \langle \hat{n}_i(t_w) \rangle_a \langle \hat{n}_j(t_w) \rangle_a]$. Using the mapping Eq. (31) we have, for $i \neq j$, $\langle \hat{n}_i(t_w) \hat{n}_j(t_w) \rangle_a = \frac{1}{4} \langle \hat{n}_i(t_w) \hat{n}_j(t_w) \rangle_c$. However, the diagonal contributions $i = j$ in this sum yield $\langle \hat{n}_i(t_w) \hat{n}_i(t_w) \rangle_a = \langle \hat{n}_i(t_w) \rangle_a = \frac{1}{2} \langle \hat{n}_i(t_w) \rangle_c$. Keeping this in mind one readily shows that $C_{e,A}(t_w, t_w) = \frac{1}{4} [C_e(t_w, t_w) + c(t_w)]$ with $c(t_w) = \langle \hat{n}_i(t_w) \rangle_c \sim 1/\sqrt{\pi t_w}$ as usual. This identity is indeed satisfied by Eqs. (115,118). While we found $C_{d,A}(t, t_w) \approx \frac{1}{2} C_d(t, t_w)$ for defect correlations in the regime $\Delta t \ll t_w$, the energy fluctuations are related by $C_{e,A}(t, t_w) \approx r_0 C_e(t, t_w)$ with $r_0 = 1 + 1/\sqrt{2} \approx 1.71$. Interestingly, in the opposite

regime $\Delta t \gg t_w$ we have from Eqs. (116,119) that $C_{e,A}(t, t_w) \approx r C_e(t, t_w)$ with the same nontrivial ratio $r = 3\pi/(6\pi - 16) \approx 3.31$ as for the defect correlations. ||

5.2. Energy-Temperature Response

By similar arguments as for the correlation one sees that the normalised energy response to a field acting uniformly on all sites i of the system is given by $R_e(t, t_w) = \sum_n R_n(t, t_w)$. Using the decomposition of $R_n(t, t_w)$, Eq. (68), we again discuss the asymmetric, $R_e^{(a)}(t, t_w) = \sum_n R_n^{(a)}(t, t_w)$, and symmetric, $R_e^{(s)}(t, t_w) = \sum_n R_n^{(s)}(t, t_w)$, parts separately.

5.2.1. Asymmetric Perturbation Summing $R_n^{(a)}(t, t_w)$, Eq. (76), over n and using the convolution property Eq. (A.5) gives

$$R_e^{(a)}(t, t_w) = \partial_{t_w} e^{-2t} [I_0 + I_1](2t) + \Delta_e^{(a)}(t, t_w) = 0. \quad (120)$$

The first term in Eq. (120) is independent of t_w and hence the derivative vanishes trivially. It can be shown that the subdominant correction $\Delta_e^{(a)}(t, t_w)$ also vanishes exactly, so that altogether $R_e^{(a)}(t, t_w) = 0$. With hindsight this result is obvious: when applied to all sites, the asymmetric perturbations of the local diffusion rates cancel. We remark that the same is true for the analogous response function $R_{e,A}(t, t_w)$ in DLPA studied in Ref. [20].

5.2.2. Symmetric Perturbation The sum over $R_n^{(s)}(t, t_w)$, Eq. (83), follows again straightforwardly using the convolution property Eq. (A.5). Here we find

$$R_e^{(s)}(t, t_w) = -e^{-2t} [I_0 - I_2](2t) + \Delta_e^{(s)}(t, t_w). \quad (121)$$

The first term is exactly $\partial_t c(t) = -e^{-2t} [I_0 - I_2](2t)$ with $c(t)$ as given in Eq. (44). This result is easily explained: first, since the response is normalised by $1/N$ it measures changes in the defect concentration $c(t) = (1/N) \sum_i \langle \hat{n}_i(t) \rangle$, the latter being just the normalised version of the energy. Now consider the effect of the corresponding symmetric perturbation. When applied locally it increases the diffusion rates between sites $i - 1 \rightleftharpoons i \rightleftharpoons i + 1$. Thus, in the global case, all diffusion rates are increased and the perturbation essentially speeds up the dynamics of the system. This is equivalent to saying that the system gains some extra time δt to evolve and therefore $R_e^{(s)}(t, t_w) = [c(t + \delta t) - c(t)]/\delta t = \partial_t c(t)$. In the aging regime this gives

$$R_e^{(s)}(t, t_w) \sim \partial_t c(t) \sim -\frac{1}{2\sqrt{\pi} t^{3/2}}. \quad (122)$$

|| We note that the ratio r coincides with the absolute value of the asymptotic FDR X_d^∞ , Eq. (108). For defect observables this originates from the fact that $\partial_{t_w} C_{d,A}(t, t_w) \sim 1/(2\pi t^2)$ in DLPA for $t \gg t_w$, see Eq. (99), scales in the same way as $R_d^{(s)}(t, t_w) \sim -1/(2\pi t^2)$ in DLPC from Eq. (106). Likewise for the energy $\partial_{t_w} C_{e,A}(t, t_w) \sim 1/(2\sqrt{\pi} t^{3/2})$ in DLPA for $t \gg t_w$ according to Eq. (119) matches the scaling of $R_e^{(s)}(t, t_w) \sim -1/(2\sqrt{\pi} t^{3/2})$ in DLPC from Eq. (122) below. However, this seems to be a mere mathematical coincidence with no obvious physical implications.

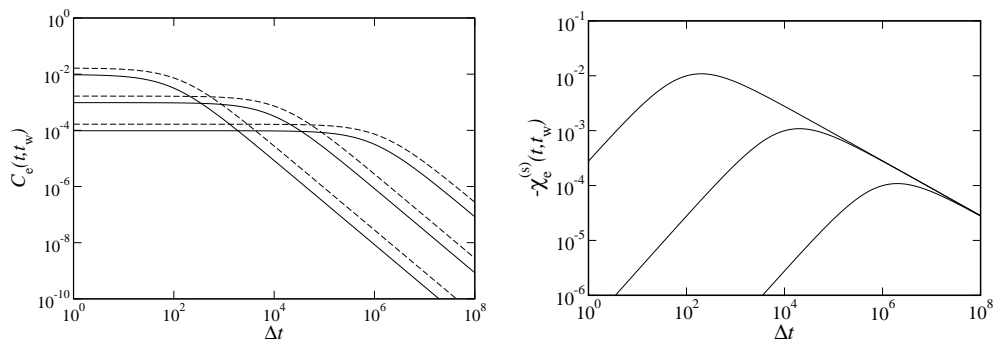


Figure 3. Left panel: scaling form of the normalized two-time energy correlation $C_e(t, t_w)$, Eq. (114), in the FA model for $t_w = 10^2, 10^4$ and 10^6 (full lines) and, for comparison, the corresponding DLPA result Eq. (117) at the same values of t_w (dashed lines). Right panel: scaling plots of the energy-temperature step response $-\chi_e(t, t_w) = -\chi_e^{(s)}(t, t_w)$ obtained from Eq. (122) for $t_w = 10^2, 10^4$ and 10^6 from top to bottom, respectively.

The global symmetric perturbation represents globally reduced energy barriers in the activated dynamics of the FA model, thus there is accelerated relaxation and a negative response. The scaling $\chi_e^{(s)}(t, t_w) \sim -(t - t_w)/(2\sqrt{\pi}t^{3/2})$ follows immediately from Eq. (122) and is shown in Fig. 3. It crosses over from $\chi_e^{(s)}(t, t_w) \approx -\Delta t/(2\sqrt{\pi}t_w^{3/2})$ for $\Delta t \ll t_w$ to $\chi_e^{(s)}(t, t_w) \approx -1/(2\sqrt{\pi}\Delta t)$ when $\Delta t \gg t_w$.

The above reasoning applies for $\Delta t \gg 1$ where the second term in Eq. (121) is subdominant. For small Δt , it cannot be neglected, and accounts for deviations arising from the fact that the perturbation does not increase all rates: that is, coagulation rates are left unchanged. Since coagulation processes are the only ones that can give an instantaneous decrease of the energy, the instantaneous response must then in fact vanish, $R_e^{(s)}(t_w, t_w) = 0$, and this can be verified from Eq. (121) by explicitly evaluating $\Delta_e^{(s)}(t_w, t_w)$.

5.3. FDR and FD plot

By combining the results derived in this section one obtains the FD plot and FDR presented in Fig. 4. Consistently with our expectations [20, 60, 61] a nontrivial limit FD plot exists for the global energy observable in the FA model. It defines the scaling form $X_e(t, t_w) \sim X_e(t_w/t)$ of the associated FDR. Since the energy-temperature step response χ_e is negative, the FD plot lies below the $\tilde{\chi} = 0$ axis. Because also the impulse response R_e is negative the slope of the plot, and thus the energy FDR $X_e(t, t_w)$, are likewise *negative* throughout.

As for the local defect observable it is crucial to use the correct parameterization of of the FD plot, with the observation time t fixed and $t_w \in [0, t]$ the running parameter [59, 60]. Had we kept t_w fixed and parameterized the plot with t , the non-monotonic shape of $\chi_e(t, t_w) = \chi_e^{(s)}(t, t_w)$ shown in Fig. 3 would have led to a non-monotonic FD plot, incorrectly suggesting a sign change in the FDR $X_e(t, t_w)$. Only

when parameterized with t_w does the slope of the FD plot correspond to the FDR X . The introduction of no-field methods for the measurement of step response functions [62, 63] has made it feasible to generate such FD plots with relative ease in numerical simulations.

Visually the limit FD plot in Fig. 4 appears to be a straight line, but this in fact not the case. The slope becomes steeper from left to right and correspondingly the FDR X_e retains a dependence on the ratio t_w/t , c.f. Fig. 4. The latter is easily derived from the scaling of $R_e^{(s)}(t, t_w)$, Eq. (122), and that of $\partial_{t_w} C_e(t, t_w)$ from Eq. (114), and has the explicit form

$$X_e(u) = - \left\{ \frac{2}{(1+u)^{3/2}} \left[1 + \frac{2}{\pi} \arcsin u \right] + \frac{2}{\pi u} \left[\frac{(1-u)^{3/2}}{1+u} - \frac{\arcsin \sqrt{u}}{\sqrt{u}} \right] \right\}^{-1}, \quad (123)$$

where $u = t_w/t$. The slope of the limit FD plot at the origin is given by $X_e(t_w/t \rightarrow 1) = -(1 + \sqrt{2}) \approx -2.41$. This means that there is no quasi-equilibrium regime, a feature that seems to be generic for global observables, at least in coarsening systems [20]. More importantly, the asymptotic energy FDR X_e^∞ is obtained by taking the opposite limit $t_w/t \rightarrow 0$, and this gives

$$X_e^\infty = \lim_{u \rightarrow 0} X_e(u) = -\frac{3\pi}{6\pi - 16} \approx -3.307. \quad (124)$$

So indeed $X_d^\infty = X_e^\infty$: the asymptotic FDRs of local and global observables are identical [20, 35, 38, 60, 61]. As for the case of local defect observables our results will be exact to leading order for the FA model in the long-time limit; this includes all aging expansions, the limit FD plots and the expressions for $X_e(u)$ and X_e^∞ . Again, finite time data are included in Fig. 4 only to give an indication of the speed of convergence (for free fermion DLPC) to the asymptotic scalings. ¶

While interesting in itself, the robustness of $X^\infty = X_d^\infty = X_e^\infty$ is also rather useful from a practical perspective: accurate measurement of X^∞ in simulations based on the local defect observable is quite difficult as is clear from the FD plot in Fig. 2: the aging properties of C_d and χ_d are disguised by quasi-equilibrium contributions. For the global energy observable, on the other hand, a nontrivial limit FD plot exists, see Fig. 4, and can be probed directly in simulations. Indeed, we have recently carried out such simulations for the FA model and the results are in very good agreement with the theoretical predictions set out above [38].

6. Summary and Discussion

In this paper we have analysed the nonequilibrium fluctuation-dissipation (FD) behaviour of the one-dimensional FA model after a quench to low temperature. The dynamics in this regime is essentially a diffusion-coagulation process, and the link from this to diffusion-annihilation and thence to the Glauber-Ising chain allowed us

¶ We remark that the nonuniform convergence of $X_e(t, t_w)$ in the right panel of Fig. 4 is due to short-time contributions from $\Delta_e^{(s)}(t, t_w)$ in Eq. (121) which yield $R_e^{(s)}(t_w, t_w) = 0$ and hence $X_e(t_w, t_w) = 0$.

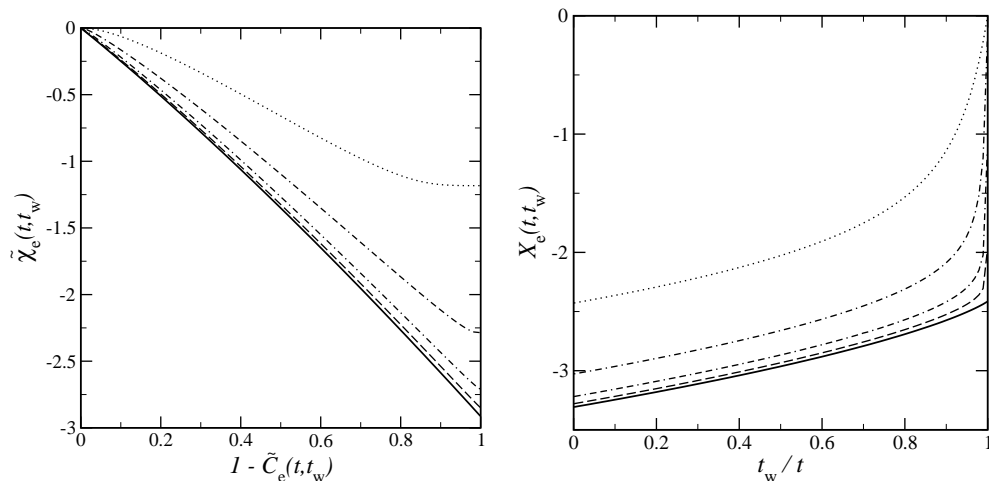


Figure 4. Left: Normalised FD plot for the energy. The curves correspond to $t = 10^1$ (dotted), 10^2 , 10^3 , 10^4 and ∞ (full curve) with $t_w \in [0, t]$. Finite time data is obtained by numerical evaluation [58] of the full expressions (111) and (121) while the limit curve follows from Eqs. (114,122). Right: Plots of $X_e(t, t_w)$ versus t_w/t for $t_w = 10^1$ (dotted), 10^2 , 10^3 , 10^4 and ∞ (full curve) obtained from the same equations.

to obtain exact scaling results for the correlation and response functions of defects (mobile regions). We were thus able to resolve a puzzle posed by simulation results [21]: the equilibrium behaviour suggested by numerical FD plots of local quantities is only apparent and hides the underlying non-equilibrium effects. The root cause of this is that the regime where the FDR X differs from unity becomes progressively compressed, as times grow, into a corner of the plot. The FDR X itself is nevertheless a nontrivial scaling function of t_w/t . A second key observation was that local and global defect observables give consistent values of the asymptotic FDR X^∞ , reinforcing the generality of our findings for Ising models [20, 60, 61].

An unexpected result of our analysis is that X^∞ is, in fact, negative. This seems counter-intuitive, certainly if one were to try to interpret T/X^∞ as an effective temperature. However, our analysis showed that the negative value of X^∞ can be traced to the behaviour of the response functions, which are sensitive to the *activated* nature of the dynamics [17, 22, 38]. In the global response function, for example, the applied perturbation corresponds effectively to an increase in temperature. In equilibrium this should *increase* the energy. However, in the out-of-equilibrium dynamics the increased temperature speeds up the relaxation of the energy and thus actually *decreases* its value. In agreement with this intuition, we found a negative (impulse) response $R_e(t, t_w)$. Except at short time differences, it is t_w -independent and just given by the time derivative (at time t) of the unperturbed energy relaxation: the small “extra time” provided by the perturbation has the same effect whenever it is applied.

As regards the wider applicability of our results, we have repeatedly emphasised that the two-time correlation functions we have calculated are exact for generic diffusion-limited pair coagulation (DLPC) processes in one dimension, in the long-time scaling

limit. In the regime of small time differences, $\Delta t = t - t_w \ll t_w$, the behaviour is easily rationalized in terms of non-interacting random walkers. Rather less trivial is the behaviour in the opposite regime $t \gg t_w$. Here we find scaling exponents identical to those for diffusion-annihilation (DLPA) processes, but quantitatively different scaling functions. The propagators used to derive these results are exact for the free fermion DLPC and DLPA processes. Higher order propagators could be obtained immediately from the results in [54] and would form the key to analysing multi-particle and/or multi-time correlations in these processes for general initial conditions.

Our response function results are similarly exact for generic DLPC processes in the long-time limit. Here one has to bear in mind, however, that the way the perturbation by the field enters can vary between models. For example, a DLPC process can be realized as the $q \rightarrow \infty$ limit of the one-dimensional Potts model [55] with Hamiltonian $\mathcal{H} = -\sum_i \delta_{s_i, s_{i+1}}$, $s_i \in \{1, \dots, q\}$, and Glauber rates. At low temperatures the domain walls $n_i = 1 - \delta_{s_i, s_{i+1}}$ have DLPC dynamics with coagulation rate 1 and diffusion rate from bond $(i, i+1)$ to $(i+1, i+2)$ of $1/2 + (h_i + h_{i+1})/(4T)$, with the fields h_i conjugate to n_i . This is precisely the asymmetric part of the perturbation that we found in the FA model; the symmetric part, which in the FA case contains all the activation effects, is absent. Because the asymmetric part of the response behaves similarly in DLPC and DLPA, see comments at the end of Sec. 4.2.1 and Sec. 5.2.1, the FD behaviour is then also like in the annihilation case [20], with an asymptotic FDR $X^\infty = 0$.

Our results also shed light on a recently proposed method for measuring response functions in spin systems [64] and deriving associated nonequilibrium FD-relations. This approach assumes a specific asymmetric form of the perturbation, which in the FA case effectively amounts to discarding the symmetric part of the response. As the discussion of the Potts model above shows, this has drastic effects; in particular, it would lead one to conclude incorrectly that the FA model has a vanishing asymptotic FDR instead of the nontrivial value $X^\infty = -3\pi/(6\pi - 16)$. The method of [64] and the out-of-equilibrium FD-relation derived from it can therefore not be accepted as generally valid.

It is worth noting that our result for the response function of the FA model has recently been quoted as being consistent with the predictions of a generalized form of local scale invariance [65]. This is indeed so for the global response Eq. (122) but *not* for the local response function Eqs. (104,106), because of the factors of $t + t_w$ that appear in both the symmetric and asymmetric parts. This suggests to us that the agreement in the global case is coincidental and cannot be taken to imply that the FA model genuinely fits into the local scale invariance scheme.

In future work it will be interesting to extend our calculations to the response and correlation of Fourier modes of the defect density, which contain the global (energy) observable as the limiting case of zero wavevector. Such Fourier decompositions have proved valuable in the past in, e.g., Ising models [20] and also lend themselves naturally to a comparison with field-theoretical results in two or more dimensions [38]. Taking a broader view, it will be essential to establish how generic our finding of negative response functions is: the link to activated dynamics suggests that, once properly measured using,

e.g., global observables, negative responses may be much more common than previously thought. The corresponding negative FDRs, while not having a natural interpretation in terms of effective temperatures [5], may be worthwhile in and of themselves in elucidating the nature of the activated dynamics.

Appendix A. Special Functions

Modified Bessel functions of integer order are most conveniently defined through the Fourier series of their generating function

$$e^{t \cos(\varphi)} = \sum_{n=-\infty}^{\infty} I_n(t) e^{in\varphi} = I_0(t) + 2 \sum_{n=1}^{\infty} I_n(t) \cos(n\varphi). \quad (\text{A.1})$$

Note that useful resummation properties follow immediately. For instance, setting $\varphi = 0$ gives $e^t = I_0(t) + 2 \sum_{n=1}^{\infty} I_n(t)$. An explicit integral representation for the $I_n(t)$ is obtained by Fourier transformation,

$$I_n(t) = \int_0^{2\pi} \frac{d\varphi}{2\pi} \cos(n\varphi) e^{t \cos(\varphi)}. \quad (\text{A.2})$$

Elementary properties of the $I_n(t)$ apparent from these equations are $I_{-n}(t) = I_n(t)$, $I_n(-t) = (-1)^n I_n(t)$ and $I_n(0) = \delta_{n,0}$. One shows that further

$$\partial_t I_n(t) = \frac{1}{2} [I_{n-1}(t) + I_{n+1}(t)], \quad (\text{A.3})$$

$$\frac{n}{t} I_n(t) = \frac{1}{2} [I_{n-1}(t) - I_{n+1}(t)], \quad (\text{A.4})$$

which we use extensively throughout the main text. From Eq. (A.1) we obtain the convolution property

$$I_m(t_1 + t_2) = \sum_{n=-\infty}^{\infty} I_n(t_1) I_{m-n}(t_2). \quad (\text{A.5})$$

The asymptotic behaviour of the modified Bessel functions of fixed and finite order n in the limit $t \rightarrow \infty$ is given by [57]

$$e^{-t} I_n(t) \sim \frac{1}{\sqrt{2\pi t}}, \quad (\text{A.6})$$

whereas, if we simultaneously take $t, n \rightarrow \infty$ with n^2/t fixed,

$$e^{-t} I_n(t) \sim \frac{1}{\sqrt{2\pi t}} e^{-n^2/(2t)}. \quad (\text{A.7})$$

Another important function in our analysis is $H_n(t)$, a full characterization of which can be found in [54]; here we only summarize those features that are pertinent to the present context. First, $H_n(t)$ may be defined through

$$H_n(t) = \frac{1}{2} \int_0^t d\tau e^{-\tau} [I_{n-1}(\tau) - I_{n+1}(\tau)]. \quad (\text{A.8})$$

Clearly $H_{-n}(t) = -H_n(t)$ is odd in n and hence $H_0(t) = 0$. Remarkably, all functions $H_n(t)$ can be decomposed into modified Bessel functions via the recursion

$$H_{n+1}(t) = H_n(t) + \delta_{n,0} - e^{-t} [I_n(t) + I_{n+1}(t)], \quad (\text{A.9})$$

which applies for $n \geq 0$ and is derived by expressing $H_{n+1}(t) - H_n(t)$ via Eq. (A.8) and noting that the integrand becomes $\frac{1}{2} e^{-\tau} [-I_{n-1}(\tau) + I_n(\tau) + I_{n+1}(\tau) - I_{n+2}(\tau)] = -\partial_\tau e^{-\tau} [I_n(\tau) + I_{n+1}(\tau)]$. Iterating Eq. (A.9) we then have $H_1(t) = 1 - e^{-t} [I_0(t) + I_1(t)]$, $H_2(t) = 1 - e^{-t} [I_0(t) + 2I_1(t) + I_2(t)]$, etc. As a consequence $H_n(t \rightarrow \infty) = 1$ for all $n \geq 1$. The latter is useful for deriving asymptotic expansions of $H_n(t)$: we rewrite Eq. (A.8) as $H_n(t) = 1 - \frac{1}{2} \int_t^\infty d\tau e^{-\tau} [I_{n-1}(\tau) - I_{n+1}(\tau)]$ so that $\tau \geq t$ in the integrand. Then, using Eqs. (A.4), (A.6) and (A.7) we obtain that at fixed $n \geq 1$ and for $t \rightarrow \infty$

$$H_n(t) \sim 1, \quad (\text{A.10})$$

while for $t, n \rightarrow \infty$ with n^2/t fixed,

$$H_n(t) \sim \Phi\left(\frac{n}{\sqrt{2t}}\right) \quad \text{where} \quad \Phi(z) = \frac{2}{\sqrt{\pi}} \int_z^\infty du e^{-u^2}. \quad (\text{A.11})$$

This defines the symbol $\Phi(z) = 1 - \text{erf}(z)$ for the complementary error function. It remains to add that beyond Eqs. (A.8) and (A.9) there is yet another useful representation for the function $H_n(t)$, viz.

$$H_{i_2-i_1}(2t) = 1 - \sum_{j_1 < j_2} G_{i,j}^{(2)}(t), \quad (\text{A.12})$$

which applies for $i_1 < i_2$. Consistently with the notation elsewhere the sum in Eq. (A.12) runs over both $j_1, j_2 \in \mathbb{Z}$, but subject to the constraint $j_1 < j_2$. In order to establish the validity of Eq. (A.12) we substitute the Green's function Eq. (48), set $j_2 = j_1 + m$, shift $j = j_1 - i_1$ and abbreviate $n = i_2 - i_1 \geq 1$, which yields

$$H_n(2t) = 1 - e^{-2t} \sum_{m=1}^{\infty} \sum_{j=-\infty}^{\infty} [I_j(t) I_{j+m-n}(t) - I_{j-n}(t) I_{j+m}(t)].$$

After convolving the modified Bessel functions using Eq. (A.5) this expression reduces to $H_n(2t) = 1 - e^{-2t} \sum_{m=1}^{\infty} [I_{m-n}(2t) - I_{m+n}(2t)]$. The remaining summation over $m \geq 1$ is telescopic and one easily verifies that it obeys the recursion Eq. (A.9), thus proving the validity of Eq. (A.12).

Appendix B. Subdominant Responses

Here we establish subdominance of the corrections $\Delta_{i,j}^{(a/s)}(t_w, t_w)$ to the instantaneous response functions for asymmetric and symmetric perturbations. These are given by

$$\begin{aligned} \Delta_{i,j}^{(a/s)}(t_w, t_w) &= \frac{1}{4} (\mp \delta_{j,i_1} + \delta_{j,i_1-1}) \langle e | \hat{n}_{i_1-1} \hat{n}_{i_1} E_{i_1+1,i_2} e^{W^c t_w} | 1 \rangle \\ &\quad + \frac{1}{4} (+\delta_{j,i_2} \mp \delta_{j,i_2-1}) \langle e | E_{i_1,i_2-1} \hat{n}_{i_2-1} \hat{n}_{i_2} e^{W^c t_w} | 1 \rangle. \end{aligned} \quad (\text{B.1})$$

The $-$ and $+$ alternatives for the signs correspond respectively to the asymmetric case, Eq. (74), and the symmetric one, Eq. (81). To evaluate Eq. (B.1) we substitute

$\hat{n}_i = 1 - E_{i,i+1}$ as usual, which reduces the averages to combinations of the form Eqs. (40,41). Then, making use of the recursion Eq. (A.9) yields

$$\Delta_{i,j}^{(a)}(t_w, t_w) = -\frac{1}{4}A_{i,j} \varphi_{i_2-i_1}(2t_w) \quad \text{and} \quad \Delta_{i,j}^{(s)}(t_w, t_w) = \frac{1}{4}B_{i,j} \varphi_{i_2-i_1}(2t_w), \quad (\text{B.2})$$

with $A_{i,j}$ and $B_{i,j}$ the coefficients defined below Eq. (73) and (80), respectively, and

$$\varphi_n(2t_w) = e^{-2t_w}[I_0 - I_2](2t_w)H_n(2t_w) + e^{-4t_w}[(I_0 + I_1)(I_{n-1} - I_{n+1})](2t_w). \quad (\text{B.3})$$

At large t_w and fixed n^2/t_w this scales like

$$\varphi_n(2t_w) \sim \frac{1}{2\sqrt{\pi}t_w^{3/2}} \left[\Phi\left(\frac{n}{2\sqrt{t_w}}\right) + \frac{2}{\sqrt{\pi}} \frac{n}{2\sqrt{t_w}} \exp\left(-\frac{n^2}{4t_w}\right) \right], \quad (\text{B.4})$$

which reduces correctly to the scaling $\varphi_n(2t_w) \sim 1/(2\sqrt{\pi}t_w^{3/2})$ for large t_w but fixed n . Comparison to the leading contribution in the asymmetric response obtained from Eq. (75) shows that $\Delta_{i,j}^{(a)}(t_w, t_w)$ is uniformly – with respect to $n = i_2 - i_1$ – subdominant and may therefore be ignored. The situation is somewhat different for the symmetric case: at fixed n and large t_w the leading term in the symmetric response Eq. (82) scales like $\mathcal{O}(n/t_w^{3/2})$ whereas $\Delta_{i,j}^{(s)}(t_w, t_w) = \mathcal{O}(1/t_w^{3/2})$. For small $n \geq 1$ contributions from $\Delta_{i,j}^{(s)}(t_w, t_w)$ cannot be neglected, however, the leading term in $R_{i,j}^{(s)}(t_w, t_w)$ grows linearly with n and thus quickly dominates $\Delta_{i,j}^{(s)}(t_w, t_w)$. Specifically, once $n^2/t_w = \mathcal{O}(1)$ we have $\Delta_{i,j}^{(s)}(t_w, t_w) = \mathcal{O}(1/t_w^{3/2})$ while the leading term in Eq. (82) scales like $\mathcal{O}(1/t_w)$. Altogether contributions from $\Delta_{i,j}^{(s)}(t_w, t_w)$ to the long time scaling of the symmetric instantaneous response become negligible when $n = i_2 - i_1 \gg 1$.

References

- [1] Ediger M D, Angell C A, and Nagel S R, 1996 *J. Phys. Chem.* **100** 13200
- [2] Young A P (ed), 1998 *Spin Glasses and Random Fields* (New York: World Scientific)
- [3] Cugliandolo L F and Kurchan J, 1993 *Phys. Rev. Lett.* **71** 173
- [4] Cugliandolo L F and Kurchan J, 1994 *J. Phys. A: Math. Gen.* **27** 5749
- [5] Cugliandolo L F, Kurchan J, and Peliti L, 1997 *Phys. Rev. E* **55** 3898
- [6] Franz S, Mezard M, Parisi G, and Peliti L, 1998 *Phys. Rev. Lett.* **81** 1758
- [7] Fisher D S and Huse D A, 1986 *Phys. Rev. Lett.* **56** 1601
- [8] Sillescu H, 1999 *J. Non-Cryst. Solids* **243** 81
- [9] Ediger M D, 2000 *Annu. Rev. Phys. Chem.* **51** 99
- [10] Glotzer S C, 2000 *J. Non-Cryst. Solids* **274** 342
- [11] Andersen H C, 2005 *Proc. Nat. Acad. Sci.* **102** 6686
- [12] Crisanti A and Ritort F, 2003 *J. Phys. A: Math. Gen.* **36** R181
- [13] Crisanti A, Ritort F, Rocco A, and Sellitto M, 2000 *J. Chem. Phys.* **113** 10615
- [14] Viot P, Talbot J, and Tarjus G, 2003 *Fractals* **11** 185
- [15] Nicodemi M, 1999 *Phys. Rev. Lett.* **82** 3734
- [16] Garrahan J P and Newman M E J, 2000 *Phys. Rev. E* **62** 7670
- [17] Depken M and Stinchcombe R, 2005 *Phys. Rev. E* **71** 065102
- [18] Krzakala F, 2005 *Phys. Rev. Lett.* **94** 077204
- [19] Fielding S and Sollich P, 2002 *Phys. Rev. Lett.* **88** 050603
- [20] Mayer P, Berthier L, Garrahan J P, and Sollich P, 2003 *Phys. Rev. E* **68** 016116
- [21] Buhot A and Garrahan J P, 2002 *Phys. Rev. Lett.* **88** 225702

- [22] Jack R L, Berthier L, and Garrahan J P, 2006 *J. Stat. Mech.* P12005
- [23] Barrat A and Berthier L, 2001 *Phys. Rev. Lett.* **87** 087204
- [24] Castillo H E, Chamon C, Cugliandolo L F, and Kennett M P, 2002 *Phys. Rev. Lett.* **88** 237201
- [25] Bellon L, Ciliberto S, and Laroche C, 2001 *Europhys. Lett.* **53** 511
- [26] Fredrickson G H and Andersen H C, 1984 *Phys. Rev. Lett.* **53** 1244
- [27] Ritort F and Sollich P, 2003 *Adv. Phys.* **52** 219
- [28] Garrahan J P and Chandler D, 2002 *Phys. Rev. Lett.* **89** 035704
- [29] Garrahan J P and Chandler D, 2003 *Proc. Nat. Acad. Sci.* **100** 9710
- [30] Jung Y J, Garrahan J P, and Chandler D, 2004 *Phys. Rev. E* **69** 061205
- [31] Toninelli C *et al*, 2005 *Phys. Rev. E* **71** 041505
- [32] Whitelam S, Berthier L, and Garrahan J P, 2004 *Phys. Rev. Lett.* **92** 185705
- [33] Whitelam S, Berthier L, and Garrahan J P, 2005 *Phys. Rev. E* **71** 026128
- [34] Jack R L, Mayer P, and Sollich P, 2006 *J. Stat. Mech.* P03006
- [35] Calabrese P and Gambassi A, 2005 *J. Phys. A: Math. Gen.* **38** R133
- [36] Buhot A, 2003 *J. Phys. A: Math. Gen.* **36** 12367
- [37] Mayer P and Sollich P, 2005 *Phys. Rev. E* **71** 046113
- [38] Mayer P *et al*, 2006 *Phys. Rev. Lett.* **96** 030602
- [39] Van Kampen N G, 1981 *Stochastic Processes in Physics and Chemistry* (Amsterdam: North-Holland)
- [40] Henkel M, Orlandini E, and Santos J, 1997 *Ann. Phys.* **259** 163
- [41] Täuber U C, Howard M, and Vollmayr-Lee B P, 2005 *J. Phys. A: Math. Gen.* **38** R79
- [42] Henkel M, Orlandini E, and Schütz G M, 1995 *J. Phys. A: Math. Gen.* **28** 6335
- [43] Krebs K, Pfannmüller M P, Wehefritz B, and Hinrichsen H, 1995 *J. Stat. Phys.* **78** 1429
- [44] Merolle M, Garrahan J P, and Chandler D, 2005 *Proc. Nat. Acad. Sci.* **102** 10837
- [45] Jack R L, Garrahan J P, and Chandler D, 2006 *J. Chem. Phys.* **125** 184509
- [46] Garrahan J P *et al*, 2007 cond-mat/0701757
- [47] Graham I S, Piche L, and Grant M, 1993 *J. Phys.-Cond. Mat.* **5** L349
- [48] Follana E and Ritort F, 1996 *Phys. Rev. B* **54** 930
- [49] Schulz M and Trimper S, 1997 *Int. J. Mod. Phys. B* **11** 2927
- [50] Ben-Avraham D, 1998 *Phys. Rev. Lett.* **81** 4756
- [51] Masser T O and Ben Avraham D, 2001 *Phys. Rev. E* **64** 062101
- [52] Glauber R J, 1963 *J. Math. Phys.* **4** 294
- [53] Santos J E, 1997 *J. Phys. A: Math. Gen.* **30** 3249
- [54] Mayer P and Sollich P, 2004 *J. Phys. A: Math. Gen.* **37** 9
- [55] Derrida B and Zeitak R, 1996 *Phys. Rev. E* **54** 2513
- [56] Zhong D X and Ben-Avraham D, 1995 *J. Phys. A: Math. Gen.* **28** 33
- [57] Gradshteyn L S and Ryzhik I M, 2000 *Table of Integrals, Series, and Products* (New York: Academic Press)
- [58] Mayer P, 2004 *PhD Thesis* King's College London
- [59] Sollich P, Fielding S, and Mayer P, 2002 *J. Phys.-Cond. Mat.* **14** 1683
- [60] Mayer P, Berthier L, Garrahan J P, and Sollich P, 2004 *Phys. Rev. E* **70** 018102
- [61] Pleimling M, 2004 *Phys. Rev. E* **70** 018101
- [62] Chatelain C, 2003 *J. Phys. A: Math. Gen.* **36** 10739
- [63] Ricci-Tersenghi F, 2003 *Phys. Rev. E* **68** 065104
- [64] Lippiello E, Corberi F, and Zannetti M, 2005 *Phys. Rev. E* **71** 036104
- [65] Henkel M, Enss T, and Pleimling M, 2006 *J. Phys. A: Math. Gen.* **39** L589